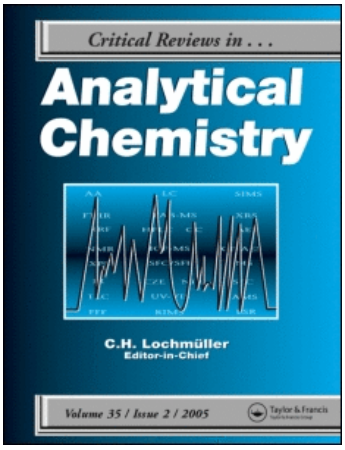

Critical Reviews in Analytical Chemistry
Publication details, including instructions for authors and subscription information:
http://www.informaworld.com/smpp/title~content=t713400837

Charge Transfer Device Detectors and Their Applications to Chemical Analysis

Jonathan V. Sweedler[a]
[a] Department of Chemistry, University of Illinois, Urbana, IL

To cite this Article Sweedler, Jonathan V.(1993) 'Charge Transfer Device Detectors and Their Applications to Chemical Analysis', Critical Reviews in Analytical Chemistry, 24: 1, 59 — 98
To link to this Article: DOI: 10.1080/10408349308048819
URL: http://dx.doi.org/10.1080/10408349308048819

Critical Reviews in Analytical Chemistry, 24(1):59–98 (1993)

Charge Transfer Device Detectors and Their Applications to Chemical Analysis

Jonathan V. Sweedler

University of Illinois, Department of Chemistry, 1209 W. California St., Urbana, IL 61801

Referee: Alexander Scheeline, School of Chemical Sciences, University of Illinois, Urbana, Illinois, 61801.

ABSTRACT: In the last 20 years, charge-transfer device detectors (CTDs) have evolved from small analog shift registers to the most common imaging detector available today. CTDs are a category of array detectors that include the charge-coupled device (CCD) and the charge-injection device (CID). Modern devices can have a peak quantum efficiency in excess of 80%, read noises of < 5 e, dark count rates of 1 e/h per detector element and formats as large as 4096 by 4096 elements. The operation and characteristics of CTDs are described, with the readout methods useful in scientific applications emphasized. The application of CCDs and CIDs to a number of fields of chemistry are reviewed, including the fields of Raman spectroscopy, molecular fluorescence, molecular absorption, atomic emission and X-ray detection. Trends in the application of CTDs and their expected impact on a number of areas of chemical analysis are featured.

KEY WORDS: charge-transfer device (CTD), charge-coupled device (CCD), charge-injection device (CID), multichannel detection, spectroscopy, instrumentation.

I. INTRODUCTION

Photons are one of the most powerful and versatile probes of a system available to the measurement scientist. In imaging systems, sub-micron spatial resolution can be combined with chemical selectivity to give information on both a molecule's location and its chemical environment. In analytical applications, spectroscopic techniques based on absorption, fluorescence, Raman, or emission offer unmatched sensitivity or specificity, and can help unravel the composition of complex samples. Optical spectroscopy can even detect single molecules in rigorously controlled situations.[1-4]

The purpose of this paper is to review current trends in the use of charge-transfer device (CTD) detectors as they are applied to the field of chemical analysis. CTDs are two-dimensional array detectors that collect and store the photogenerated charge and then measure the quantity of charge present. CTDs get their name because charge detection is accomplished by *transferring* the charge from a collection region to a detection region. In a CTD, the charge-transfer process is accomplished by changing the voltages applied to a series of electrodes overlaying the collection region.

Almost all CTDs manufactured today are based on silicon.[5] Although a silicon CTD can have a significant responsivity from the soft X-ray region to the very near-infrared, there is an intense effort to extend the wavelength range of CTDs further into the infrared using nonsilicon substrates such as InGaAs, MCT, and PtSi. Although current

1040-8347/93/$.50

infrared CTD performance greatly lags behind silicon CTD performance, infrared CTD characteristics are improving rapidly. However, because it is beyond the scope of this paper to describe infrared CTDs, interested readers are referred to several recent overview articles on such detectors.[6-8]

Although the two major subclasses of CTDs, the charge-injection device (CID) and the charge-coupled device (CCD), have many similarities, they have very different performance characteristics and modes of operation. Therefore, CID and CCD operation and electrooptical characteristics are treated separately. One of the goals of this review is to describe current performance characteristics of CTDs in order that readers can select the CTD most other appropriate to their particular application. Unlike other common analytical detectors, CTDs are available with an unbelievable variety of characteristics and prices, ranging from the CCDs found in commercial $200 video cameras to large 16 million detector element, high-speed CCD systems with prices over $100,000. Thus, it is impractical to purchase a single "general purpose" CCD system, and the scientist is required to make a number of decisions regarding performance characteristics. In addition, understanding device characteristics allows a researcher to evaluate complete systems designed for other applications. Does a spectroscopist need the high-end CCD systems offered by Astromed, Princeton Instruments, or Photometrics Ltd. costing more than $25,000, or can a $1500 system designed for amateur astronomy be used? Such low-end systems still have thermoelectrically cooled detectors to reduce dark current, acquire 12-bit data, include a direct interface to a PC, and include image control software.[9,10] Although most analytical chemists are familiar with the pertinent electrooptical characteristics of single-channel detectors such as read noise, dark current, quantum efficiency, dynamic range, and response time, the two-dimensional nature of CTDs adds a number of additional and important parameters, such as array format, specialized readout modes, charge-transfer efficiency, and intra- and interscenic dynamic range. The large number of readout modes and important characteristics offered by CTDs reflect the considerable flexibility offered by these detectors.

II. HISTORICAL PERSPECTIVE

The CCD detector concept was developed in 1970 by Boyle and Smith of Bell Laboratories,[11] and the first experimental device was described by Amilio et al.[12] Although the intended use of the CCD was in the areas of analog memory and shift registers, their potential as an imaging detector was quickly realized. Michon and Burke of General Electric Company developed the first 32 by 32 element CID in 1972.[13] Because of the commercial and military potential of the CID technology, a 100 by 100 element CID, complete with scanners, was soon developed. Both the first commercially available CID from General Electric and the first CCD from Fairchild were introduced in 1973. The first scientific uses of the CCD and the CID were in the area of astronomy, both occurring in 1976.[14,15] Although astronomers were the first to demonstrate the imaging performance of CTDs in scientific applications, chemists were the first to demonstrate their utility in a spectroscopic measurement. In 1979, Ratzlaff used a linear CCD for molecular absorption,[16] and in 1983, Denton demonstrated the use of a CID for atomic emission spectroscopy.[17]

Advances in CTD technology have been driven by two different groups with contrasting needs.[18] The first group consisted of electronics manufacturing companies such as AT&T, RCA, Fairchild, GE, and Texas Instruments; these companies supported the early development of CTDs in an effort to design and manufacture solid-state television cameras. This work resulted in the commercial manufacture of CTDs for surveillance, document scanners, and home video cameras.

The second group was lead by astronomers, engineers, and physicists, who

needed a more sensitive and more photometrically accurate detector than photographic film. These researchers convinced NASA and NSF to fund the development of specialized CTDs for use in space probes, satellites, and astronomical observatories. These efforts resulted in the first CTDs designed specifically for scientific applications, and greatly furthered the fundamental understanding of CTD imagers. These scientists and engineers also designed the first "scientific" CTD camera systems. These scientific camera systems are fundamentally different from ordinary video camera systems: the data are digitized at 12 to 20 bits of precision, the digitization rate is slowed in order to accomplish this, the detector is cooled to reduce dark current, special signal conditioning circuits are employed to reduce detector noise, and special operating modes are built-in to allow read modes tailored to specific applications.

Because of this early development, an extremely wide range of CTD detectors is available with differing formats, wavelength ranges, electrooptical characteristics, and a wide variety of specialized readout modes. Today, CTDs are the most common electronic imaging detector manufactured. The American Chemical Society's *Chemical Abstracts* lists over 800 articles utilizing CTD detectors, with most of the articles appearing since 1985. CTD detectors can have over a 90% peak quantum efficiency, a high responsivity from the soft X-ray region to the near-infrared, dark count rates that allow integrations for many hours, and a read noise that is equivalent to < 1 e. Thus, CTDs are the first imaging detectors that combine the integrating characteristics and high spatial resolution of photographic film with a sensitivity that rivals, and in some cases exceeds, that offered by a single-channel photomultiplier tube.

III. CTDs: OPERATION, ARCHITECTURE, AND CHARACTERISTICS

CTDs are solid-state multichannel detectors and, as such, share a number of optical properties with other silicon array detectors such as photodiode arrays (PDA). CTDs accumulate charge as light strikes them, much like photographic film. This is in contrast to the photomultiplier tube, which produces a single current proportional to the "instantaneous" photon flux at the photocathode. An individual detector in a CTD array consists of several conductive electrodes overlying an insulating layer that forms a series of metal-oxide semiconductor (MOS) capacitors. The insulator separates the electrodes from the doped silicon region used for photogenerated charge storage. There is a wide variety of architectures and geometries used depending on the device and manufacturer.

In a silicon lattice, a photon of sufficient energy can create a mobile electron and a mobile vacancy (hole) in the lattice. These two will quickly recombine unless they are separated by the application of external potential fields. In a CTD, a series of electrodes overlying the silicon is used to create the electric fields needed to separate and store either the photogenerated holes or electrons. Importantly, the amount of photogenerated charge is proportional to the number of photons striking the detector. The amount of charge is measured by either moving it from the detector element where it accumulates to a charge-sensing amplifier (intercell charge transfer) or by moving it within a detector element and sensing the voltage change induced by the movement (intracell charge transfer). Charge-coupled devices employ the intercell readout, and charge-injection devices use intracell readout. Both CCDs and CIDs share a number of common traits, including the inherent quantum efficiency offered by the silicon substrate and the same basic dark-current floor from the silicon lattice. However, the readout modes, formats, and read noise are very different for the two classes of devices.

The majority of CCDs and CIDs are designed for use in imaging applications. Linear arrays are typically used in line scan applications and two-dimensional arrays are primarily intended for direct imaging. The design (number and size of pixels, register, and

preamp design) and architecture (number of phases, illumination method, and buried or surface channel) generally reflects the intended readout mode and application. Although a device operated according to its intended readout mode may prove useful in spectroscopy, improvements can generally be made by operating the device in a so-called specialized readout mode. Fortunately, the nature of CCDs and CIDs is such that the flexibility exists to operate them in widely varying ways. For example, readout speeds may be greatly reduced to improve noise performance and device clocks may be altered to affect readout of only specific portions of the device. Because the design and architecture of CIDs and CCDs affect their performance in scientific applications, selection of a device that offers both the desired spectral properties (wavelength response, noise, linearity, and full well) and that will operate in the desired readout mode is essential. As the number and variety of applications of CCDs and CIDs in science and engineering expands, more and more devices are being designed and produced with operation in one or more of the specialized modes in mind. Although the detector arrays themselves are flexible in terms of readout modes and operating parameters, most complete imaging systems are not. Thus, one must be careful in the purchase of complete systems to ensure that they support the desired readout strategies.

A. Charge-Coupled Devices

There is an extraordinary range of CCDs that have been fabricated by a large number of manufacturers over the last 20 years. Because each manufacturer uses slightly different technology and offers devices tailored for slightly different applications, a short description of CCD operation is followed by discussion of the important operating characteristics available from CCDs. The interested reader is referred to several overview articles describing in much greater detail the operation of these detector arrays.[7,19-22]

1. Architecture

As previously stated, the CCD is a metal-oxide semiconductor structure that stores photogenerated charge carriers. Overlying the silicon is a series of conductive electrodes. When an incident photon penetrates to the silicon substrate and forms a hole–electron pair, the electron migrates under the influence of a potential applied to one of the overlying gate electrodes and is stored there until charge readout. By correctly biasing the multiple overlying electrodes, the photogenerated charge is constrained to the element where it is generated. The number of phases indicates the number of overlying electrodes for which the voltage can be independently controlled for each detector element.

Once the integration period is over, the charge is shifted from the photoactive area to a charge-sensing amplifier located at a corner of the array. A single (or in some cases, several) output node is located at the edge of the array, and the charge information is shifted to this amplifier in a sequential manner. It is the ability to transfer the charge from the sensing element to a specialized low-capacitance output node, and hence to eliminate high-capacitance multiplexed architecture, that differentiates CCDs from CIDs, PDAs, and other array detectors. The extremely small capacitance of the input of the output amplifier allows CCDs to achieve their ultralow read noise.

The transfer of charge from the imaging area to the output amplifier occurs by shifting the charge from detector element to adjacent detector element. The applied potentials in a detector element must be controlled in several distinct regions in order for this to be accomplished. Figure 1 demonstrates the charge transfer process for a three-phase CCD; at least one of the three potential well regions in the detector element is always held low (collapsed) so that a barrier exists to prevent charge from spilling into the next adjacent element. Shifting the location of this barrier causes charge to migrate.

In Figure 1, potential well diagrams are shown below each drawing. These diagrams

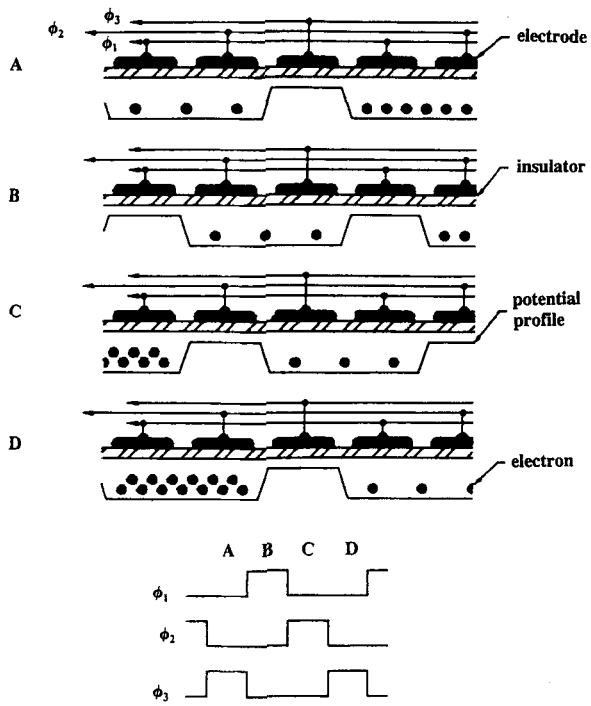

FIGURE 1. Diagram of a three-phase CCD's showing the charge-integration and charge-transfer processes at four different time states. The voltages applied to the three independently controllable phases are switched between a high and a low level, forcing the charge to migrate to the right. (The voltages applied to each phase for each time are shown in the bottom of the figure.) (Reprinted from Bilhorn, R.B.; Sweedler, J.V.; Epperson, P.M.; Denton, M.B., *Appl. Spectrosc.* **1987**, *41*, 1117. With permission.)

indicate the "favorableness" of a region for the storage of charge; the more energetically favorable a region is, the deeper the potential well shown in the diagram. Although the figures show the charge filling up from the bottom, in surface channel CCDs the initial charge resides near the silicon–silicon dioxide interface. Almost all CCDs manufactured today use a buried channel architecture, in which an implant under the surface of the CCD makes it more energetically favorable for the charge to reside away from the interface. This minimizes the contact of the charge with the silicon-silicon dioxide interface and thus improves device operation. In such a potential well diagram, as an electrode is made more positive, the well gets deeper (and charge may spill into the deeper well from adjacent areas). Similarly, as an electrode is made more negative, charge contained under that electrode may be "forced" into a different region as shown in Figure 1.

The overall organization and readout of a two-dimensional CCD is illustrated in Figure 2. As can be seen, the array consists of a serial register and a parallel (imaging region) register. The charge in all columns of the parallel register is shifted downward into the serial register one row at a time. As each row is shifted into the serial register, the charge from individual elements is shifted to the left into the readout amplifier. Thus, for each parallel shift, the entire serial register is read out. Fixed potential barriers are created between columns to prevent charge migration across the parallel register. These barriers, or channel stops, can be created by the diffusion of a p-type material or by the use of a thick oxide over the area of the channel stop.

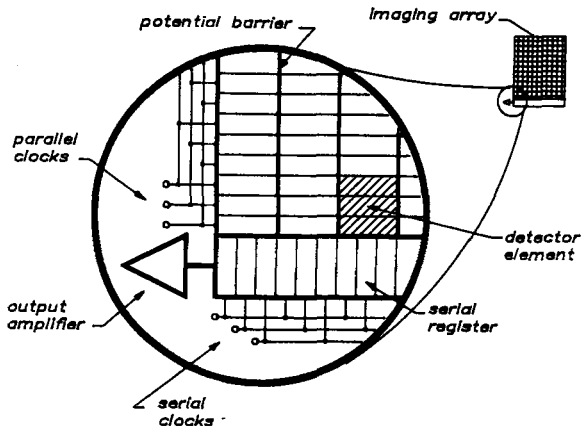

FIGURE 2. Layout of a typical three-phase CCD showing the imaging area, serial register, and readout amplifier. The photogenerated charge is shifted downward in parallel to the serial register. The charge in the serial register is then shifted left to the on-chip amplifier and measured. (Reprinted from Sweedler, J.V.; Bilhorn, R.B.; Epperson, P.M.; Sims, G.R.; Denton, M.B., *Anal. Chem.* **1988**, *63*, 242A. With permission.)

In addition to the three-phase architecture, the transfer of charge can be accomplished by using anywhere from one to four independently controllable phases. One can use fewer than three by employing implants or variations in oxide thickness to create steps in the potential wells that force the

desired charge movement. Devices that use single-phase (uniphase, or Texas Instrument's [TI] virtual phase) and two-phase devices are commercially available. Four-phase devices are also common because they lead to a simpler manufacturing process. Although the transfer of charge from the region of collection to a low-noise amplifier allows the extremely low read noise of CCDs, it requires an extremely efficient transfer of charge. In addition, using a single amplifier limits the maximum readout rate; several manufacturers offer four-quadrant devices with readout amplifiers in all four corners to speed up the readout process (i.e., this can be thought of as four arrays manufactured together with no dead zone between the arrays). Several high-speed CCDs have been made for military applications with readout amplifiers on each column. This greatly adds to the cost and increases the readout speed.

In what follows, the major aspects of CCD performance are described. In each case, the optimum performance obtained for CCDs is described as well as more common architectures and specifications.

2. Charge Generation and Collection

One of the most important characteristics of an optical detector is the quantum efficiency (QE). Although a responsivity in the 400 to 900-nm range is available from almost every detector, silicon CCDs are available that respond from the 1- to 1000-nm region.[19,20] For photons with a long absorption length (i.e., wavelengths greater than 500 nm or less than 1 nm), the QE depends on the thickness of the photosensitive volume. For intermediate wavelengths with relatively short photon absorption lengths in silicon and silicon dioxide, the QE depends largely on the transparency, reflectivity, and surface conditions of the layers that overlie the photosensitive element. Because of the large variety of CCD architectures and technologies, the QE response in these wavelength regions varies dramatically depending on device architecture. Because the UV to soft X-ray and the near-infrared regions are important to many applications, great efforts have gone into optimizing the response of CCDs to these energies.

Conceptually the easiest to understand method of enhancing ultraviolet QE is the application of a down-converting fluorescent coating to the surface of the CCD. Such a coating absorbs the UV photons and reemits them at wavelengths to which the CCD responds. Even with highly efficient coatings, however, many of the photons will be reemitted in directions away from the CCD surface and so the QE in the ultraviolet will be significantly less than the peak visible QE. Because such coatings are much less expensive than the alternatives (described later), a number of CCD manufacturers and several complete systems vendors offer such coatings. A potential concern of a down-converting coating involves the long-term stability when exposed to ultraviolet photons. Several coatings have been shown to be remarkably stable; for example, the lumagen coating offered by Photometrics Ltd. is stable for long periods when a cooled CCD is exposed to vacuum UV photons.

A second method of optimizing the short wavelength QE is to eliminate the overlying gate electrodes over a portion of the imaging area and use an implant to allow charge integration and storage (i.e., similar to TI's virtual phase devices). When looking at Figure 1 for the three-phase device, one can imagine one phase held constant (using an implant) and shifting the charge by the correct application of voltages to the remaining two phases. Because one of the phases of the CCD has no overlying gate electrodes and can have a thin oxide, it can respond in the UV region (and have an enhanced visible QE). Recently, Janesick and co-workers designed and tested such a device.[23] In their implementation, the open phase was 12 μm wide and the two remaining phases were each 3 μm wide, so that two thirds of the surface area of the CCD had no overlying gate structure. With this structure, the CCD still maintained excellent charge-transfer characteristics and had the higher QE as expected. I expect to see more CCDs manufactured using this process in the near future.

The minimization of overlying gate structure is also the reason for the high QE of TI's virtual phase devices.[24]

A third method of increasing the QE of the CCD in the UV region is the technique of back-side illumination.[19] In this case, the CCD is thinned to 10 to 30 μm and illuminated from the side opposite the gate structure, as illustrated in Figure 3. The appropriate thinning depth is critical because the photogenerated electrons must migrate under the influence of the applied electric fields from the electrodes located on the front of the device. A device that is too thin will suffer from a loss of visible and red QE because these photons can pass through the entire device before being absorbed. Optimizing the QE of a back-side device is further complicated by the presence of a slight positive field at the back surface. Thus the first photogenerated electrons "stick" to the back surface and will not be collected by the electric field maintained by the electrode on the front surface of the device. This secondary problem can be reduced by using a so-called flash gate, UV flooding, electron gun flooding or other techniques to leave a slight negative charge on the back (illuminated) surface to repel the photogenerated electrons toward the front surface.[19,20,23] These methods can produce devices with measured QEs that are amazingly high (see the QE curves in Figure 4). However, problems with long-term stability and reproducibility have prevented these techniques from being widely applied. One of the biggest problems with back-side-illuminated CCDs is commercial availability and cost; because of this, optimized back-side-illuminated devices may not be options for many users.

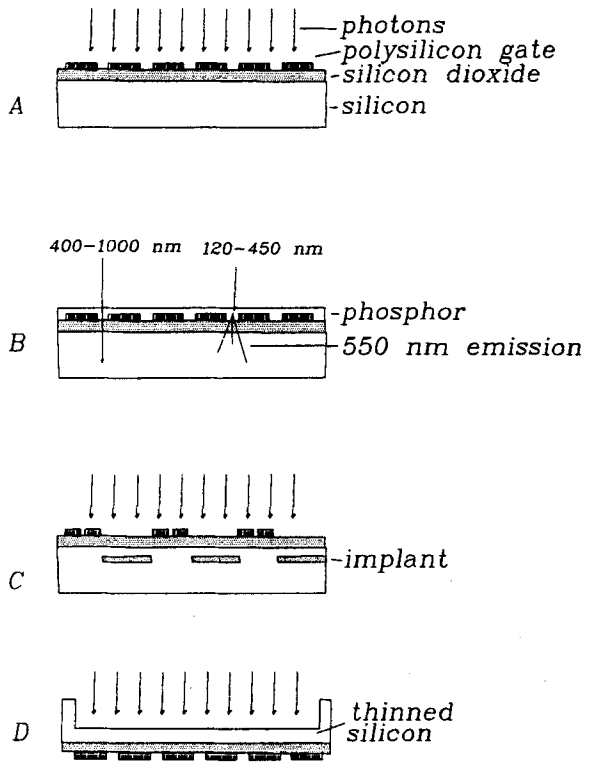

FIGURE 3. Cross sectional diagrams of several different CCD architectures demonstrating the methods used to enhance ultraviolet QE. Shown are (A) standard thick CCD, (B) a phosphor coated CCD, (C) an open phase CCD, and (D) back-side-illuminated CCD.

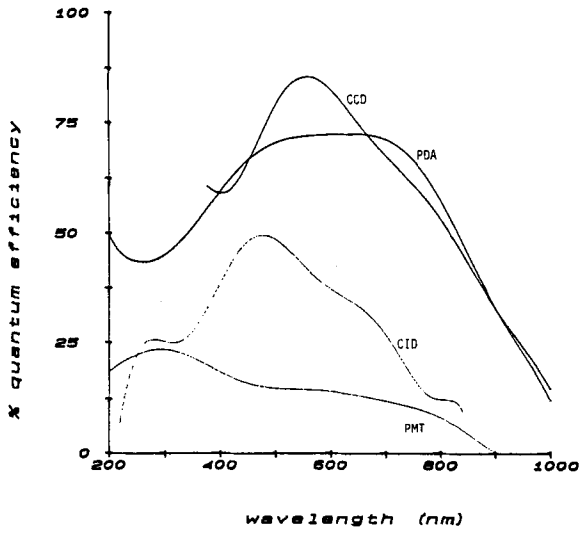

FIGURE 4. Quantum efficiency versus wavelength for several representative detectors: a Texas Instruments 800 by 800 CCD, a General Electric 244 × 388 CID, a Reticon RL 1024S PDA, and a Hammamatsu GaAs opaque photocathode available in PMT's. (Reprinted from Sweedler, J.V.; Bilhorn, R.B.; Epperson, P.M.; Sims, G.R.; Denton, M.B., *Anal. Chem.* **1988**, *63*, 242A. With permission.)

Regardless of the spectral region of interest, one of the first goals in obtaining a high QE is getting the photon into the CCD. In fact, several CCDs have a "*100% internal QE*" in the 200 to 500-nm range;[19] once the photon makes it into the CCD, the resulting

electrons will be collected. Because silicon has a very high index of refraction, large reflection losses occurs at the surface of these devices. The QE can be increased over limited wavelength regions by the use of the appropriate antireflection coating. The presence of thin layers of different materials on the CCD surface complicates the selection of an antireflection coating. Unfortunately, a single antireflection coating is not available that increases the QE over the entire 100 to 1000-nm region. As illustrated in the QE curves shown in Figure 4, the QE of a back-side-illuminated antireflection coated CCD can be over 80% over a limited wavelength range.

3. Charge Transfer

Once the electrons are generated and collected in the detector element, the next major step is to transfer this packet of charge to the output amplifier. Charge Transfer Efficiency (CTE) is a measure of the ability of the device to transfer the charge from one potential well to the next. For current CCDs, this process can be amazingly efficient; for a properly operated and manufactured device, the CTE is much greater than 0.99999 per transfer (a CTE of "five 9s"). The amount of charge left in a packet for a three-phase CCD is given by:[25]

$$N_{\text{final}} = (N_{\text{orig}})(\text{CTE}_{\text{serial}})^{3X}(\text{CTE}_{\text{parallel}})^{3Y}$$
$$(\text{CTE}_{\text{parallel-serial}})(\text{CTE}_{\text{serial-amplifier}})$$

where N_{final} and N_{orig} are the number of electrons in the final and original charge packet, and X and Y are the number of detector elements in the serial and parallel regions that the charge has to transfer through before reaching the on-chip amplifier. For a three-phase, 2048 element square array with a six 9s CTE, charge in the far corner of the array must be transferred through 2048 elements (or under 6144 gates) in both the parallel and serial registers. For this CCD, 120 electrons are lost from a 10,000 electron packet into the first trailing element. The CTE is dependent upon the parallel and serial clock levels, the temperature of the CCD, and the amount of charge being transferred. The most serious limitation to achieving high CTE from low light level images is the loss of charge to what is termed the spurious potential pocket.[19,25] The amount of charge trapped is a very small fraction of full well, so smearing is only observed at very low light levels. Much greater detail on CTE is provided in References 7, 19, 20, and 25.

While CTEs have been improving with new device refinements, available CCD arrays also have been getting larger, and so CTE can still be a concern. Now that 4K by 4K area sensors and 8K linear CCDs are available with read noises of only a few electrons, the device CTE needs to be very close to unity if CTE losses are not to limit device performance. Recently, CTEs of 0.99999999 (eight 9s) have been recorded for the best CCDs operated under ideal circumstances.[23] This CTE corresponds to a single electron being left behind from a 10,000 electron packet transferred from the far corner of the same three-phase CCD used in the foregoing example. As other devices are manufactured with the refinements of these high CTE CCD devices, charge-transfer losses in even large arrays should become insignificant.

In addition to the transfer of charge down a column (in the parallel imaging region) or in the serial register, the charge needs to make two unique single transfers from the parallel to the serial register, and from the serial register to the output amplifier. Because of the different geometries involved, the transfer efficiency for these transfers may be much lower than the efficiency for the serial and parallel register. (On the other hand, only a single transfer is required.) Some CCDs suffer from additional problems during the parallel to serial transfer that impact on their use in scientific applications. For example, several early CCDs suffered from charge-trapping effects, in which some of the first charge transferred from the parallel to the serial registers was not measured.[26,27] Because these CCDs were commonly used for ultralow light level Raman spectroscopy, this

effect caused detector-induced band-shape distortions, which are a great concern because the significance of the results often depends on subtle changes in band shape. Harris[26] has recently described a quantitative investigation into charge-trapping effects on Raman spectra for the Thomson CCD. For a user of CCDs prone to charge-trapping problems, the output can be seriously distorted at low illumination levels and various corrective measures need to be implemented. However, almost no modern CCD suffers from detectable charge-trapping problems. This example illustrates that careful selection of a CCD is important to avoid such problems for low light level applications.

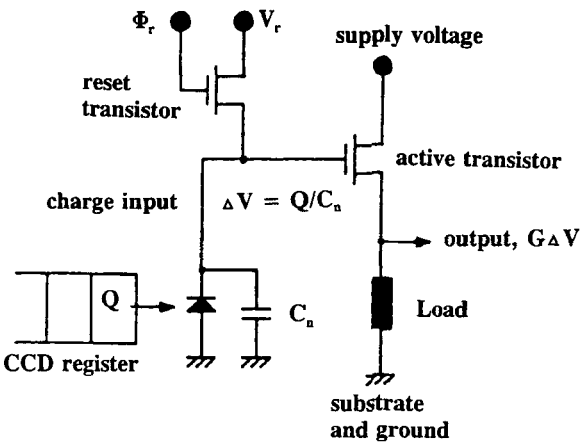

FIGURE 5. A schematic diagram of a common charge-sensing circuit used with CCDs. (Adapted from Burt, D.J., *Nucl. Instrum. Phys.* **1991**, *A305*, 565. With permission.)

4. Charge Readout

Once the charge is transferred to the output amplifier of the CCD, the next important task is to accurately and precisely measure the amount of charge in the packet. Every time the size of a charge packet is measured, an uncertainty exists as to the actual number of charge carriers. This uncertainty represents the read noise floor of the device (there can be further contributions from dark current and other effects). Figure 5 shows a common output amplifier design for CCDs.[28] The amplifier read noise is independent of integration time and can limit the ultimate sensitivity of the device. This read noise floor is limited to approximately 2 e for the best scientific grade CCDs; read noises of 5 e are widely available, and read noises under 10 e are common. A read noise of 5 e is not the limiting noise source in almost all real-world situations with background shot noise limiting most measurements. The read noise levels mentioned previously are for CCDs operated in the "slow scan mode" with specialized readout electronics that use double-correlated sampling to eliminate the effects of KTC (switch) noise,[7] and represent readout rates of 40 to 50 kHz. Although readout rates of 100,000 elements per second sound impressive, a single read of a 1024 by 1024 CCD still requires over 10 s. As the read rate is increased, the read noise increases, so that for 1-MHz readout rates, the read noise tends to be greater than 20 e. Thus, there is a trade-off between read noise (sensitivity) and read rate. Several systems have been manufactured that allow a slow (and low-noise) mode of operation and a fast (higher noise) mode. Because such systems are uncommon, careful balancing of read noise and read rate is required.

Janesick and co-workers recently demonstrated a unique CCD readout amplifier that they termed the skipper CCD.[29] In this device, a charge-sensing amplifier similar to that found in a CID (described in succeeding text) has been incorporated into the device. In such devices, either the normal or skipper amplifiers can be used. Using the nondestructive skipper amplifier, the charge information can be read many times nondestructively, thus reducing the effective read noise. Such devices can have an overall read noise of less than 1 e, but involve an extraordinary slow readout speed. Several manufacturers have incorporated skipper amplifiers on their devices,[30] but very limited reports of their use have appeared. The Advanced Technologies Division of Photometrics Ltd. may be the only commercial manufacturer currently offering complete systems that allow the use of the skipper amplifier.

Another important contribution to the device noise can be dark current. The dark count rate of a CCD is quite high at room temperature, but can be reduced dramatically with cooling. By using a liquid nitrogen cryostat, the dark count rate can be reduced below 1 electron per element per hour, which is an insignificant rate for most applications. On the other hand, if most of the photoactive area of a CCD is "binned" together and the device used as an effective "single element" device, then the dark current from many thousands of elements is combined and the dark current again becomes significant. A question that most CCD system purchasers must address is whether liquid nitrogen cooling is required or whether thermoelectric cooling will be effective. Thermoelectric systems tend to be much less expensive but do not allow cooling to as low temperatures and so have higher dark count rates.

Recent refinements to CCD operation have allowed significant reductions to dark current at a given temperature. The most common, termed the multipinned phase (MPP), reduces the dark current by more than an order of magnitude and thus may relax CCD cooling requirements to the level where a thermoelectric cooler is sufficient.[30,31] Most of the thermally generated charge is created at interface states at the silicon-silicon dioxide interface. The MPP is a clocking technique that holds the parallel phases at a negative potential. This greatly decreases the surface dark-current components, but causes the potential wells essential for charge integration to be reduced so that the charge can spread up and down the columns. However, some CCDs are made with a built-in potential step that maintains the potential wells when the parallel phases are biased in this way, thus allowing the reduction in dark current without charge smearing. The tradeoff associated with this technique is a reduction in the full-well capacity of the device. A flexible controller allows the user to select the MPP or normal modes based on the particular scene being observed.

CCDs allow considerable flexibility in readout. Two of the most widely used capabilities are subarray readout and charge binning.[32,33] Taking advantage of these capabilities requires that the electronics controlling the CCD be able to independently operate the serial and parallel registers and, for optimum performance, that the pixel digitization routine also be under separate control. Subarray readout refers to reading out a contiguous group of pixels within the CCD array and is the simplest specialized readout mode. The operation consists of eliminating the charge barriers in the serial register while the parallel clocks are advanced to the subarray's parallel origin, thus dumping the charge that has accumulated in the array up to the origin of the subarray. Next, the barriers are reestablished in the serial register and the lines making up the subarray are shifted one at a time into the serial register. Slewing to the serial origin of the subarray is done with the summing well set to drain away charge. Once the serial origin is reached, readout commences in the normal fashion. At the end of each subarray line, the remaining charge in the serial register must also be dumped so that it is not combined with the next row when it is shifted into the serial register. For a similar reason, the remaining charge in the CCD should be cleared after the last row of the subarray is read out. If it were not, it would be combined with the charge from the next exposure. More sophisticated systems allow multiple subarrays to be read from a single exposure by keeping track of which pixels and which rows of pixels to dump.

Restricting the number of pixels that must be processed by the data system to only those that contain useful information is important to both increase the readout speed and decrease the data storage and processing time. In imaging applications, a region of interest might be established interactively from a full-frame readout before beginning an involved image acquisition sequence. In spectroscopy, a subarray might be established for the region of the detector corresponding to the illuminated portion of the spectrometer entrance slit.

A second readout mode, unique to CCDs, is charge binning. Binning involves combining photogenerated charge from adjacent pixels on the detector prior to readout. The

main reasons for binning are to improve signal-to-noise ratio (SNR), dynamic range, and readout speed.[32] Detector read noise is independent of signal level, so combining the charge from two equally illuminated pixels results in doubling the SNR in detector read-noise-limited situations. Because only a square-root improvement is achieved with conventional signal averaging, the ability to bin can be a significant advantage of the CCD. In photon shot-noise-limited situations, the expected square-root improvement is also achieved. Obviously, the trade-off with binning is loss in spatial resolution. Because dark current is binned along with signal charge, considerably better cooling is required to prevent dark-current shot noise from becoming the limiting noise source in applications where long exposure times are combined with a high degree of binning.

The process of binning involves shifting multiple rows from the parallel region to the serial register (parallel binning) or shifting multiple pixels from the serial register into the summing well (serial binning). Modern scientific CCDs are designed with binning in mind, so the serial register and summing node charge capacities generally exceed that of the parallel register.[25] However, with excessive binning, it is possible to cause blooming in the serial register or the summing node even though the exposure has been adjusted to prevent blooming in the parallel register. The combination of subarray readout and charge binning is a powerful tool for optimizing SNR, illumination requirements, integration time, and total measurement time.

One of the main advantages of binning is improving SNR when detector read noise dominates the measurement SNR. Because the read noise levels are so low in modern slow-scan CCD cameras, very little light intensity is required before the measurement becomes dominated by photon shot noise. Once this is the case, binning offers no advantage over summing or averaging in computer memory in terms of SNR, although an advantage in readout speed and convenience may be realized. Caution must be exercised when binning in high dynamic range spectroscopic applications. A common example involves one-dimensional spectroscopy, where the second array dimension is aligned along the slit. If the illumination along the slit is nonuniform, it may be possible to cause pixel saturation in one of the binned spectra without the problem occurring in the other spectra, thus complicating quantitation. Automated routines that collect spectra from multiple binning groups, detect high-energy particle events and then average the spectra to produce a result must also check for saturation or present the spectra to the user prior to averaging. Because binning may not be desirable when sufficient light is available to bring pixel intensity values into the photon shot-noise-dominated range in a measurement time that is practical and convenient, binning should only be considered when dark-current shot-noise or detector read noise begin to dominate a measurement or when measurement time can be shortened without incurring a severe SNR penalty.

The last readout mode of the CCD described here is the time delayed integration (TDI) mode. TDI involves synchronizing the movement of an image across the sensor with the CCD parallel clocks so that the photogenerated charge produced by the illumination from the scene moves with the image. Thus, all of the pixels along a column of the CCD are used to integrate charge from a point in the scene. TDI readout allows the acquisition of long image swaths from a moving scene, and is at present not commonly used in spectroscopy or scientific imaging. The technique was first developed in the mid 1970s for use in airborne reconnaissance, but since that time has been applied in document scanning and inspection applications, spectral imaging,[34,35] and analytical spectroscopy.[36] In conventional imaging a trade-off exists between field of view and spatial resolution because of the number of pixels in the imager. If resolution and field of view requirements exceed what can be achieved in a single exposure, then multiple images must be combined. TDI is a viable alternative to combining still images. TDI is a technique for creating a scanned image where a two-dimensional imager much like a linear sensor

is used to scan an image. Smearing is avoided by maintaining careful synchronization between the movement of the scene and the shifting of the charge in the CCD, and images of unlimited scan length can be collected. An improvement in sensitivity over line-scan systems is achieved that is directly proportional to the number of lines in the two-dimensional sensor in the scan direction.

5. Charge Blooming

Blooming is the spilling of charge from an illuminated detector element to adjacent elements. The onset of blooming in a CCD occurs when the maximum number of photogenerated charge carriers that can be held in an element is exceeded. Because the charge initially generated in the imaging region is transferred through several different regions before being sensed at the output amplifier, blooming can occur in several different areas of the detector.[25]

Even for low light applications, blooming performance can be important. As one example, when a CCD is used at the focal plane of a spectrograph with both intense and weak spectral lines, blooming can be the limiting factor dictating overall performance.[37] It is important to realize that the full-well capacity of the serial register can be several times larger than the parallel register, and that the summing register often has a capacity several times that of the serial register. Thus, binning can still be used in cases where several bright features are expected.[25] The channel stops in the parallel area usually prevent charge blooming across columns, and so the bloomed charge spills down the column. In many spectroscopic applications, the effects of blooming can be minimized by orienting the spectral lines with the parallel shift direction. Thus, the excess charge will bloom down the column and not into regions corresponding to other wavelengths.

Many manufacturers offer CCDs that contain antiblooming drains to prevent charge blooming. Such CCDs tend to have a slightly lower QE (because of the area taken up by the antiblooming drain). In these devices, excess photogenerated charge spills into the drain and is conducted away. While quantitative information is lost in the saturated element, the excess charge is conducted away and does not affect the charge information contained in nearby detector elements. In addition, several CCD architectures can be operated with unique clocking schemes that minimize the effects of blooming. As one example, Texas Instruments makes a family of linear CCDs that can be operated in a readout mode that greatly reduces the effects of charge blooming.[24]

6. Array Formats

CCDs are available in an amazing variety of sizes, formats, and characteristics. Table 1 lists the formats of several representative CCDs; square arrays are available in sizes from 64 by 64 elements up to arrays of 4096 by 4096 elements, and with photoactive sizes from 1 to over 2500 mm.^{2} As the area of an array increases, the number that can be manufactured on a given wafer goes down and, not surprisingly, the cost goes up. Thus, it is advantageous to use the smallest size array that can accommodate a particular application.

Linear arrays are available with up to 8196 elements. Unfortunately, most linear CTDs have small, approximately square, detector elements typically only 5 to 25 μm on a side.[24,38,39] On the other hand, linear CCDs require few overlying gate electrodes and, hence, can have higher quantum efficiencies than two-dimensional arrays.[24,38,39] Because of the small geometries, efficient use of these detectors requires image demagnification to more efficiently measure the light from a spectrograph with tall narrow slits. The image of a tall slit can be compressed with a cylindrical lens.[24] The greatest advantage of the linear CCD is in the area of cost; such a 3456 element linear array can cost $< \$100$, but complete systems optimized for low light level spectroscopic applications are just becoming available.

TABLE 1
Representative CTD Formats and Characteristics

Device	Format	Pixel size (μm)	Dark current (e / pixel / s) (°C)	Readout noise (e)	Quantum efficiency
CID Technologies					
CID17BAS	244 × 378	27 × 23	< 0.01 @ −140	50 (with NDROs)	47% at 550 nm
CID75	1 × 1	1000 × 1000	100 @ −140	120 (with NDROs)	35% at 250 mm; 34% at 440 nm
EEV					
CCD05-10	298 × 1152	23 × 23	6 @ −45	9	
CCD15-11	1024 × 256	27 × 27	3×10^{-5} @ −120 (MPP)	4	40% at 700 nm
Loral Fairchild					
FA1024L	1024 × 1024	15 × 15	3×10^{-5} @ −120 (MPP)	5	45% at 700 nm
FA4096S	4096 × 4096	7.5 × 7.5			
Kodak					
KAF-4200	2048 × 2048	9 × 9	0.02 @ −35 (MPP)	13	42% at 700 nm
KAF-1300L	1280 × 1024	16 × 16		15	40% at 700 nm
Photometrics					
PM512	512 × 512	20 × 20	3 @ −45 0.03 @ −110	5	45% at 700 nm
Tektronix					
TK512CB/AR	512 × 512	27 × 27	12 @ −45 0.01 @ −110	4	85% at 650 nm
Texas Instruments					
TC104-1	3456 × 1	10 × 10	0.1 @ −110	60	90% at 400 nm
TC-211	204 × 165	14 × 16	0.1 @ −110	20	60% at 500 nm
Thomson CSF					
7883	384 × 576	23 × 23	7 @ −45	8	40% at 700 nm

7. CCD Defects

When purchasing a CCD detector, one of the first questions asked of the user is what *quality* device is desired. What is usually meant by this question is what type and how many defects one willing to tolerate? Because there can be enormous differences in the price between a device with bad detector elements compared to a cosmetically "*perfect*" device, this question deserves some thought. Although all users would like perfect devices, some defects have little impact on the overall system performance. There are many types of defects, ranging from nonresponsive elements (a point defect) to problems with a section of a column of the CCD (a line defect). Because a problem with one of the phases in a CCD can prevent charge from transferring past the defect, many defects "block" a portion of a column. Other defects affect a group of elements and cause a dead area on the array. It is beyond the scope of this paper to review the causes and types of defects in CCDs. Readers desiring additional information should see the recent discussion by Sims.[40] For a particular CCD, the locations of the defects can be determined and the values from those elements replaced with the average of adjacent elements. An understanding of the effects of the defect as well as the requirements of an application can save considerable time, money, and frustration.

8. Cosmic Rays and High-Energy Events

Silicon CTDs respond to cosmic rays and background radiation. Because each high-energy photon creates thousands of hole-electron pairs, relatively few events are enough to seriously degrade the sensitivity

and the quality of the data unless corrections are made. Depending on a number of factors, including materials used in the construction of the CTD camera and the laboratory building, the geographic area, the altitude, the solar cycle, and other variables, exposure times as short as 1 min may be sufficient to produce a high-energy particle event that interferes with the appearance of spectra or images. Although both CIDs and CCDs respond to such high-energy events, CCDs tend to be used in low light level applications where their effects are much more troublesome. High-energy event removal is easiest when one is observing a scene that consists of low-frequency variations that are many detector elements wide, for example, typically bandwidths in molecular spectroscopy. In many Raman and other molecular spectroscopic experiments, the slit height dimension contains little high-frequency information and the spectral bands are many elements wide in the wavelength dimension. Therefore, the high-energy events can be removed by writing software routines that look at the raw CCD data for isolated spikes on a relatively smooth background.[41,42] Figure 6 shows the raw and spike-removed data from a Raman experiment.[42] While an extreme case, this figure demonstrates the importance of removing such high-energy events before analyzing the data. In many low light level situations, only a few undetected high-energy events can affect the detection limit. Binning information into large subarrays makes high energy event removal more difficult. Specifically, the redundant information offered by reading out individual detectors in a subarray individually instead of binning may be useful when long exposures are involved in aiding in the identification and removal of spurious signals produced by high-energy particle interactions with the CCD.

In instances when the focal plane of the detector contains many narrow, high-frequency features (such as looking at a star field or at the focal plane of a well focused echelle system), discriminating against those features that are spurious and those that are not is much more difficult. In such cases, multiple exposures can be taken to identify the cosmic rays and other radiation by looking for inconsistencies in the series of exposures. This method is commonly used in astronomical imaging; typically, the value of each detector element from at least three "identical" exposures are compared and all spikes are removed.

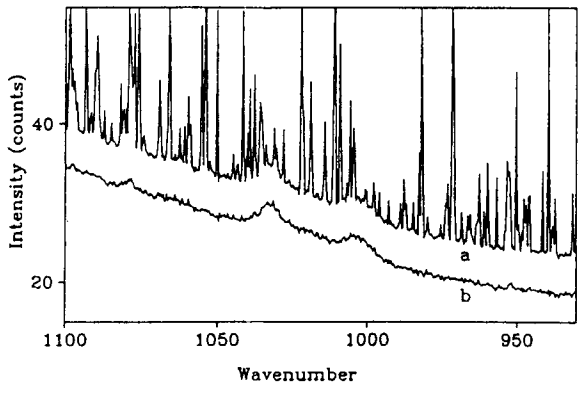

FIGURE 6. Raman spectra of pyridine adsorbed onto a smooth silver surface. Each spectrum is the average of 100 scans with 100-s integration times. (A) before and (B) after spike filtering was used to remove high-energy events. (Reprinted from Hill, W.; Rogalla, D., *Anal. Chem.* **1992**, *64*, 2575. With permission.)

B. Charge-Injection Devices

The charge-injection device is the approach to making solid-state imagers originally undertaken by General Electric Company in the early 1970s. As in the CCD, the individual detector element consists of several electrically conductive electrodes overlying a thin silicon oxide or nitride insulator. Unlike almost all commercially available CCDs, CIDs are made using an n-doped epitaxial region grown over a p-doped substrate, and hence the CID collects photogenerated holes. The overlying electrodes are biased to allow charge integration and charge collection in a similar manner to CCDs. In what follows, those aspects of CID operation that are different from CCD operation are emphasized.

1. Architecture and Readout

Charge information is measured in the detector element where it is collected rather than moved to an on-chip amplifier. Although there have been a number of modifications to the CID architecture, Figure 7 shows a simplified diagram of a single CID detector element with the two electrodes used in charge readout and charge removal. Because the charge never leaves the detector element where it is collected, CCD readout modes that allow charge combination such as binning are not applicable to CIDs. On the other hand, CIDs allow the charge information contained in a detector element to be read nondestructively (the NDRO), allow the interscenic dynamic range to be increased using random access integration (RAI), and are extremely resistant to charge blooming.

After the exposure of the CID to a scene, the quantity of charge in each pixel is measured. In CIDs, the amount of charge can be measured without removing it from the detector element, which is termed the nondestructive readout. As illustrated in Figure 7, the procedure involves shifting the photogenerated charge back and forth underneath two crossed electrodes. During charge integration, the collection electrode is biased negatively so that the photogenerated charge (holes in the CID) is collected under this electrode. For readout, the sense electrode is set to an intermediate voltage. A positive voltage pulse applied to a single collection electrode causes the photogenerated charge along the entire column to be shifted under the corresponding sense electrodes. For one selected sense electrode, the voltage change induced by the photogenerated charge is measured. A voltage proportional to the amount of stored charge is obtained by subtracting the voltage measured after the transfer of the charge to the voltage measured before the transfer, a form of correlated double sampling.

As shown in Figure 7C, the photogenerated charge is now contained under the sense electrode. By restoring the negative collection voltage, the charge returns to its original starting position. This process can be repeated and successive values of the amount

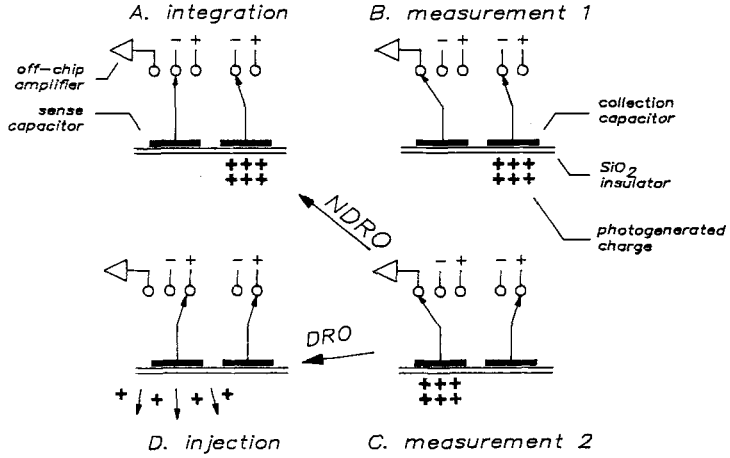

FIGURE 7. Readout of a CID showing the nondestructive measurement process. (A) The CID is in the integrate mode. (B) The first of two measurements of the potential at the sense electrode is made. (C) The charge is moved under the sense electrode and a second measurement is made. The readout process can be completed by shifting the charge back under the collection electrode (A) or injecting the charge (D) (Reprinted from Bilhorn, R.B.; Sweedler, J.V.; Epperson, P.M.; Denton, M.B., *Appl. Spectrosc.* **1987**, *41*, 1117. With permission.)

of charge can be averaged to reduce the uncertainty in each measurement. This readout mode is termed the nondestructive readout mode (NDRO) and is used to greatly reduce the uncertainty in quantitating the charge in a detector element (although it does significantly slow down the readout process). The nondestructive and destructive readout are described in greater detail by Sims and Denton[43,44] and Bilhorn and Denton.[22,45]

Until recently, CIDs were not available with on-chip amplifiers. More importantly, the large capacitance associated with the entire sense electrode and associated scanner increased the video line capacitance. This in turn contributes to the much higher read noise in CIDs; for example, the CID 17 had a single readout noise of nearly a thousand electrons.[22] Although this value can be reduced by more than a factor of 20 using multiple NDROs,[45] it is still much higher than in the read noise of modern low-noise CCDs. Several improvements in device fabrication and architecture have reduced this number considerably. A recently announced innovation is the presence of a preamplifier for every row of sense electrodes on the CID.[46] With these new CIDs, the single read readout noise can be below 100 e, and with multiple rereads, the effective read noise is predicted to be reduced below 10 e.

Figure 8 shows a schematic drawing of a two-dimensional CID. The individual detector elements are selected by the action of horizontal and vertical scanners to select the desired sense and collection electrodes. Because the horizontal and vertical scanners can be run independently, electrodes can be skipped over and small sections of the array can be accessed without the need to read out the entire array. In most devices, the scanners access rows sequentially rather than truly randomly, so many refer to this capability as pseudorandom access. The difference between the ability of a CCD and a CID to read out subarrays should be emphasized. Both devices can read a small subarray in the center of the array; however, in the case of the CID, the photogenerated charge information in the entire array is still intact, so other subarrays can be accessed.

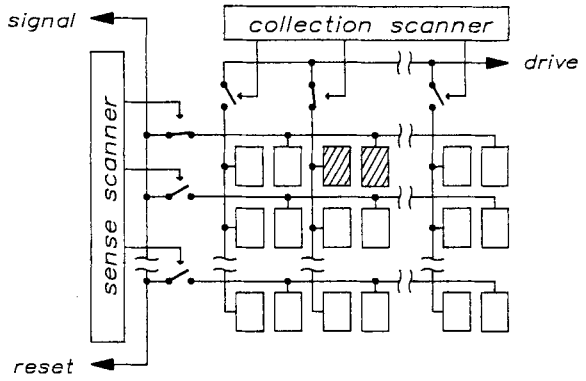

FIGURE 8. Block diagram of a two-dimensional CID showing the sense and collection scanners. These registers open and close a series of switches to connect the collection and sense electrodes to the charge drive signal and the output amplifier. The detector element at the intersection of the selected scanners is shaded and will be read during the next readout process. (Reprinted from Bilhorn, R.B.; Sweedler, J.V.; Epperson, P.M.; Denton, M.B., *Appl. Spectrosc.* **1987**, *41*, 1117. With permission.)

The nondestructive readout (NDRO) is used with the CID to reduce random noise and to extend the dynamic range of the sensor. The difference between the smallest level of charge measurable and the largest amount of charge that can be stored in a CID detector element is not sufficiently large for many applications, for example, atomic emission spectroscopy. Fortunately, excess charge does not bloom (spill into adjacent elements) in CIDs. Therefore, different exposure times can be used for different regions of the CID, *with the exposure times determined during the exposure of the CID to the source*. This procedure, called random access integration (RAI) uses NDROs during the single exposure to follow the accumulation of charge at both weak and intense spectral lines.[22,45,47] NDROs are used continuously during the exposure to determine when a high signal-to-noise measurement is possible at each spectral line. Once a high SNR can be achieved, the precise amount of charge is measured and the exposure time is recorded. The conventional dynamic range of the CID is combined with the range of integration times available for

each spectral line to produce the dynamic range needed for atomic emission spectroscopy. The RAI method is the most efficient means of measuring the intensity of a number of spectral lines because the exposure time is adjusted dynamically according to signal-to-noise requirements based on the intensity of each spectral line.

2. Available Devices

There is currently only one manufacturer of scientific CIDs, CID Technologies, Inc. CID Technologies Inc. was formed from the CID division at General Electric, so they have been involved with CID manufacture for over 20 years. Because they are a single manufacturer, there is much less variety in available CIDs compared to CCDs in terms of device architectures and formats. However, CID Technologies are currently offering a wide range of CID formats, including single element, linear, TV, and large format arrays. The formats and characteristics of several representative CIDs are listed in Table 1. All the CIDs from CID Technologies have a high intrinsic quantum efficiency from below 240 to above 900 nm. The reason for this is the relatively small fraction of the front surface of the CID covered with overlying electrodes. If a significant QE is needed below 200 nm, a down converter coating can be used as described with CCDs.[48] The dark current of a liquid nitrogen cooled CID is low enough to be difficult to measure. Because the CID tends to be used in higher light applications than CCDs and is not used in applications requiring the combining of charge from thousands of elements, CID dark current tends to be insignificant.

Based on the characteristics of CTDs described in the preceding discussion, the idea of using a single element CTD as a solid-state replacement for photomultiplier tubes has been investigated. A single element CID (the CID75) was manufactured specifically as a spectroscopic detector;[49] the prototype device had an incredible dynamic range (over 12 orders of magnitude of photon fluxes) and a high sensitivity. As illustrated in Figure 9, interdigitated electrodes were used in the CID75 to allow charge collection over a millimeter photoactive area. The major problems of hysteresis and charge clearing in the preliminary version of the CID75 have been addressed in a second generation device. The effectiveness of this second generation device as a solid-state replacement for the PMT awaits further electrooptical characterization. Whether using this device or another small CTD array, I expect that low cost solid state CTDs will replace PMTs in a number of low photon flux and high dynamic range applications.

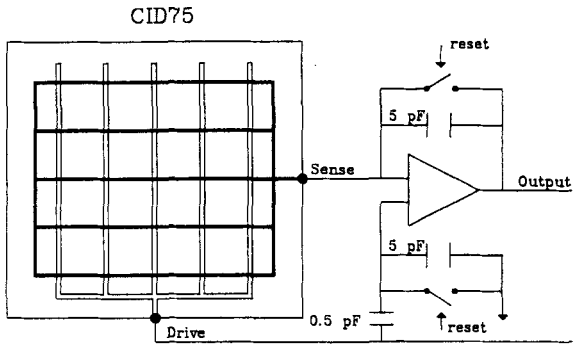

FIGURE 9. Diagram of a single element CID with a 1-mm^2 photoactive area showing the interdigitated collection and sense electrodes. The associated off-chip amplifier is also shown. (Adapted from Sweedler, J.V.; Denton, M.B.; Sims, G.R.; Aikens, R.S., *Opt. Eng.* **1987**, *26*, 120. With permission.)

IV. SURVEY OF APPLICATIONS

In the following sections, the applications of CTDs to a number of fields of chemical analysis are described. The purpose of each section is not to comprehensively review every reference of a CTD to each area, but to illustrate the variety of methods that have benefited from CTDs and to highlight emerging trends in their use. In several areas, commercial instruments are available, whereas in other areas, little has been done except proof of concept demonstrations with laboratory prototypes. Nevertheless, the application of

CTDs is increasing as more researchers use them in an expanding number of roles.

One of the greatest impediments to using a CTD for a detector in most applications is the different geometrical requirements placed on the optical system compared to systems designed to use PMTs. Although the imaging area of most CTDs is comparable to typical photocathode areas, the area available for each resolution element is *much* smaller than the photocathode area of a typical PMT. However, systems designed specifically for CTD array detectors are now available. In addition to high sensitivity, such systems offer the advantages of compact size, lack of moving parts, lower cost, and extreme ruggedness. The approaches taken to match the optical system to the CTD and performance comparisons between the various approaches are emphasized in the following text.

A. Molecular Luminescence

The sensitivity and detection limits obtainable in many luminescence experiments are constrained by a lack of signal. It is not surprising that the characteristics of CCDs that make them so well suited to microscopy and astronomical observations make them well suited to low light level luminescence measurements. In a luminescence experiment, the photons emitted as excited molecules return to the ground state are collected and detected. The term luminescence is used loosely here and can describe a number of different physical processes involved with the emission of a photon as a molecule returns to the ground state: the molecule can be excited by the absorption of a photon (fluorescence), be chemically excited (chemiluminescence), be excited by the interaction of the molecule with a high-energy particle (scintillation), accept energy from another molecule (fluorescence energy transfer), or be in the excited triplet state after an intersystem crossing (phosphorescence). The experimental details of the different approaches vary greatly. For example, a fluorescence experiment needs an excitation source and either a series of filters or a monochromator to separate the Rayleigh and Raman scatter from the fluorescence, whereas a chemiluminescent experiment system needs neither. However, the need for sensitive detection is a similar requirement in each. Although the following discussion emphasizes fluorescence and chemiluminescence, CCDs are well suited as detectors for many of the other listed processes.

Denton and co-workers were the first to demonstrate the acquisition of fluorescence spectra with a CCD.[50] In their system, the CCD was located at the focal plane of a fast, aberration-corrected spectrograph and complete emission spectra were simultaneously acquired. As shown in Figure 10, recognizable anthracene fluorescence spectra were obtained using a mercury pen lamp source down to 10^{-11} *M* anthracene concentrations with a limit of detection (LOD) of $\approx 10^{-12}$ *M*. In these experiments, optimized binning parameters were used to match the effective CCD geometry to the spectrograph slit height.[32] At the detection limit of 10^{-12} *M*, the fluorescence signal is 2800 e on a background of 260,000 e; thus, the ability to see a small signal on top of a large background determines the detection limit in this fluo-

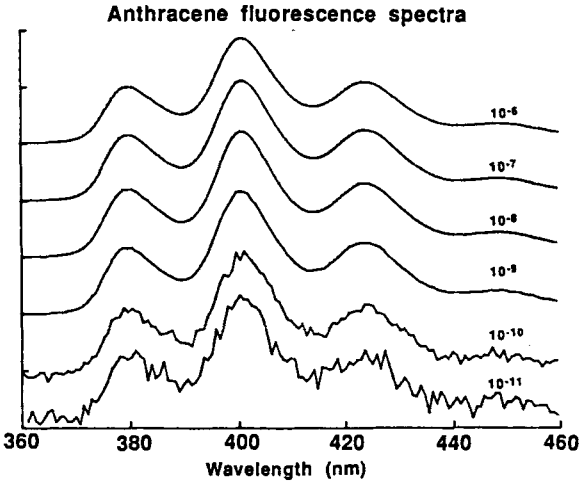

FIGURE 10. Spectra of 10^{-6} to 10^{-11} M anthracene using a Hg pen lamp excitation source. (Reprinted from Epperson, P.M.; Jalkian, R.D.; Denton, M.B., *Anal. Chem.* **1989**, *61*, 282. With permission.)

rescence experiment. Just as in molecular absorbance, significant advantages accrue to acquiring the entire fluorescence spectrum. By using the area of the largest Raman scattering band of the solvent as a reference, source fluctuations can be removed. Potentially, correcting for variations in the Raman scatter of the solvent allows a pulsed source to be used and can remove the effects of pulse to pulse variations. Of course, the wavelength information may also aid in identifying the fluorescent species, alert the user to unusual background impurities, and can be used to improve the LODs obtained using various whole-spectrum fitting methods.[51,52]

In the preceding work, one dimension of the CCD contained the slit image and the other the wavelength-resolved emission spectrum. An obvious extension is to illuminate the slit with a wavelength-resolved excitation spectrum, thus allowing the acquisition of simultaneous excitation-emission (EEM) matrices with extreme high sensitivity.[53] To be successful, careful selection of the spectrographs is important because it should be highly stigmatic (have a point to point correspondence of the entrance slit and the exit focal plane). Alternatively to acquiring complete EEMs, the second dimension can be illuminated with many fiber bundles, each of which can be from a different sample (or a different region of a single sample).[54] Thus, simultaneous spectroscopy on a number of samples becomes feasible.

Another extension of fluorescence detection is to couple a wavelength-resolved CCD system to a separation method. CCD-based fluorescence systems have been demonstrated for liquid chromatography[55] and capillary electrophoresis.[34,56,57] Figure 11A shows a schematic diagram of such a fluorescence detector for high performance liquid chromatography (HPLC), and Figure 11B shows the separation and wavelength information obtained from the system for a mixture of seven polycyclic aromatic hydrocarbons (PAHs). The emission-excitation matrix (EEM) shown in Figure 11C is for the same seven PAH mixture. This EEM demonstrates that the two wavelength axes do not contain enough information and that the HPLC separation is required to resolve the components.

The combination of capillary electrophoresis (CE) and CCD detection has received considerable attention in the last several years. CE is a separation technique where the components in the sample are electrophoretically separated in narrow bore capillaries by the application of an external electric field. Typical separation capillaries have $<$ a 50-μm inner diameter. If a laser is focused onto the capillary, the fluorescence excitation is effectively from a point or a line source, so well designed collection optics can match the source to the spectrometer slit very effectively. The first application of a CCD to CE used the CCD as a camera at the focal plane of the spectrometer. The camera, complete with a shutter, is used to take a series of pictures of the fluorescence emission from a point on the capillary as a function of time. Using this system, LODs of nanomolar concentration and attomole amounts of fluoresceinisothiocyanate (FITC)-labeled amino acids have been reported.[57] Zare and co-workers[34] demonstrated a CCD-based system that used a 2-cm observation zone (compared to the $<$ 100 μm of typical systems). Figure 12A shows a block diagram of the system, where the optics image this section of capillary onto the entrance slit of an imaging spectrograph. During the separation (whether chromatographic or electrophoretic), the analyte band moves down the capillary and its image moves across the CCD. If the CCD readout rate is synchronized with the analyte band movement, then the effective integration time is the entire time the band is in the illuminated zone. Unlike non-imaging systems, this increase in observation zone does not correspond to a decreased spatial resolution (separation efficiency). Using this TDI approach, LODs of 10^{-12} M (zeptomole amounts) of FITC-labeled amino acids are obtained.[34,35] Figure 12B shows a wavelength-resolved separation of approximately a 3-amol injection of fluorescein and sulforhodamine 101.[34] When using the TDI mode, the CCD dimension corresponding to the capillary image is used for signal integration, and the output of

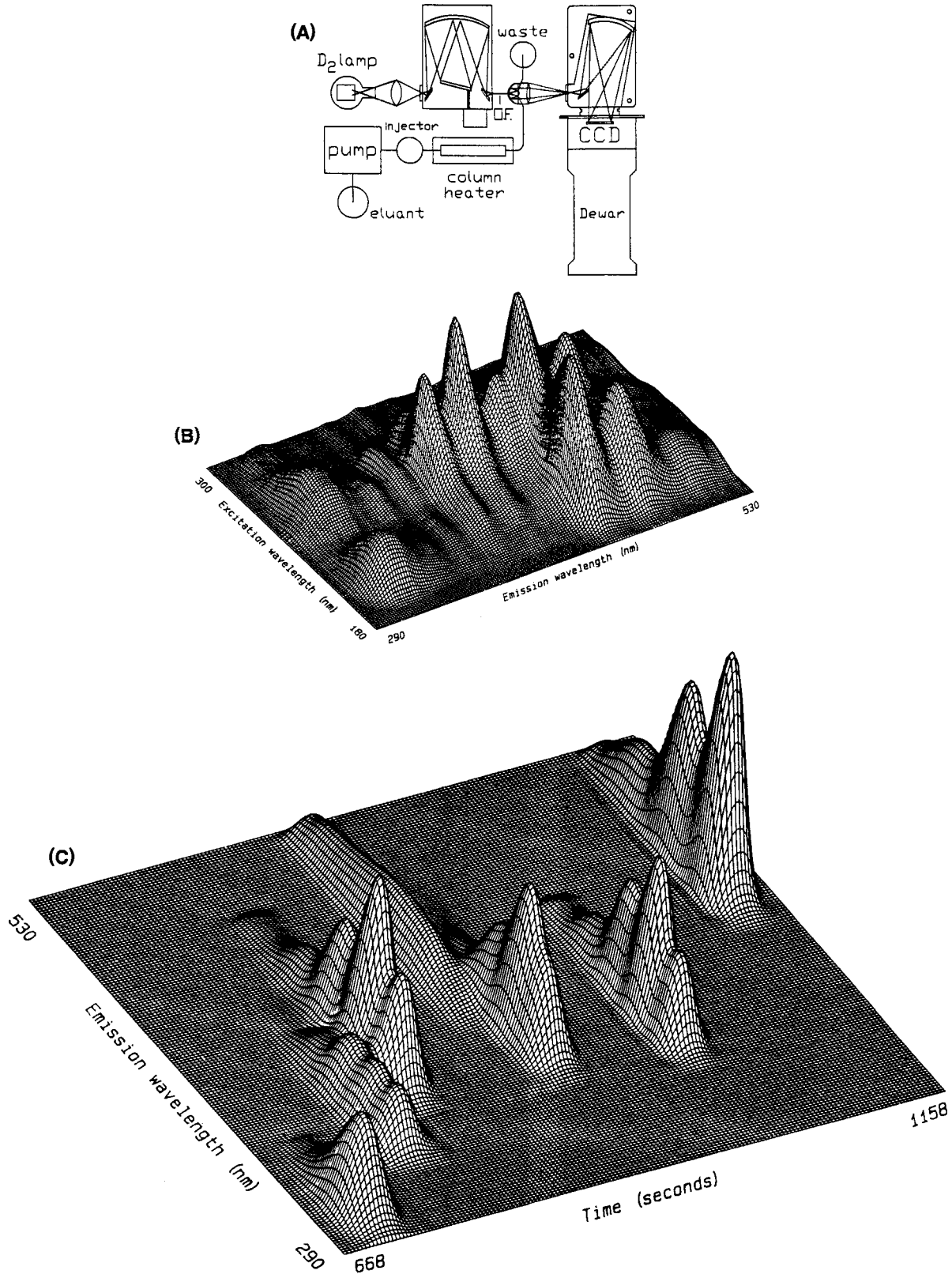

FIGURE 11. (A) The instrumental configuration for an on-line HPLC fluorescence detection system using a CCD detector. (B) Fluorescence emission-excitation matrix (EEM) of a seven PAH mixture. (C) Chromatogram of the emission spectra as a function of time obtained for the same seven PAH mixture. (Reprinted from Jalkian, R.D.; Denton, M.B., *Proc. SPIE* **1989**, *1054*, 91. With permission.)

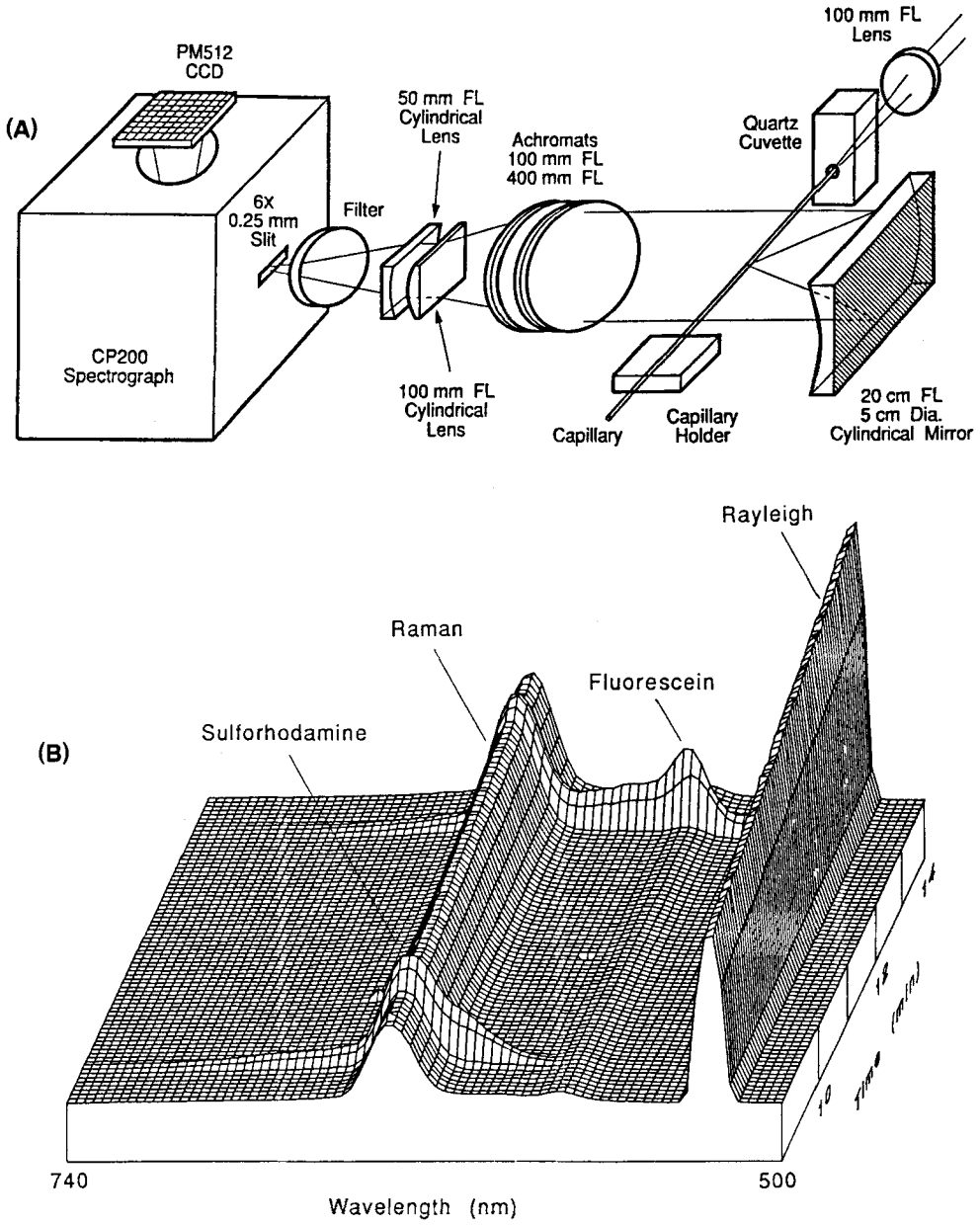

FIGURE 12. (A) Schematic diagram of the optical system used to image a 2-cm section of a capillary electrophoresis capillary onto the slit of the spectrometer. The CCD focal plane records a fluorescence spectrum from every point along the 2-cm region. (B) A TDI electropherogram of 3 amol of sulforhodamine and fluorescein. The Rayleigh and Raman scattering bands are clearly visible at all times, with the wavelength-resolved sulforhodamine and fluorescein spectra also obvious. (Reprinted from Sweedler, J.V.; Shear, J.B.; Fishman, H.A.; Zare, R.N.; Scheller, R.H., *Anal. Chem.* **1991**, *63*, 496. With permission.)

the system is an infinite series of fluorescent spectra, each of which corresponds to a several hundred micrometer wide band migrating through the observation region. Using rhodamine-based derivatizing agents, the LODs of this system improved to < 1000 tagged molecules.[58]

An important advantage of the combination of a CCD and spectrograph is the acquisition of complete emission spectra that allows multiple fluorophores to be spectroscopically resolved. Because one of the most common methods of sequencing DNA is to use different fluorophores attached to each

of the four bases making up our genetic code, such wavelength-resolved information allows the fluorophore (and hence base) to be determined based on spectral characteristics.[56,57] As previously mentioned, the wavelength information can also be used to increase the measurement precision by correcting for source fluctuations and other insta-bilities. Other benefits are the ability to test and screen many tags without the need to have specially designed filters for each fluorophore, and to detect the presence of contaminants in running buffers and solvents by the presence of background fluorescence emission.

In addition to fluorescence, the use of a CCD for luminol chemiluminescence measurements has also been reported.[59] In this system, the CCD was positioned near a reaction cell where the luminol peroxide solution is mixed with a metal-ion solution. Such a system can be used to quantitate the amount of metal ion present. To increase the dynamic range of these measurements, the CCD was divided into three regions with different binning parameters for each: one region consisting of 2 by 2 binning of 800 elements at the edge of the array for high intensity measurements, an intermediate region, and a region of over 50,000 detector elements read with 10 by 70 binning. The last region yields the highest sensitivity. All three regions are read after each exposure period and the appropriate region is selected based on the measured values of each. The effective dynamic range of the measurement is greatly increased using this method; the CCD detector used 14-bit digitization electronics but is able to quantify Cr^{3+} and Co^{3+} solutions ranging from 10^{-13} to 10^{-5} M using these multiple readout regions without prior knowledge of the signal intensity. In addition to static measurements, the chemiluminescence system also was demonstrated for liquid chromatography with LODs in the low femtomole range.[59]

One of the most obvious uses of a CCD detector is for spectroscopic imaging where the CCD is used to view an object and wavelength information is acquired using filters or spectrometers. The use of a scientific CCD as a detector for fluorescence microscopy is the most common application of scientific CCDs outside of astronomy, partly because it is straightforward to interface the 35-mm camera or C-mount video adapter on a microscope to a scientific CCD imaging system. A scientific CCD is ideally suited to fluorescence microscopy because of its geometric fidelity, extreme sensitivity, and the availability of large format arrays. In the last several years, CCDs have started to dominate digital fluorescence microscopy for both slow-scan scientific instruments[60-67] and in intensifier-video CCD combinations for high-speed applications.[68,69] In almost all cases, a series of filters is used to select both the emission and excitation wavelengths. As a further refinement, Sedat[62,70] has developed a three-dimensional optical sectioning fluorescence imaging system using CCD detection. Slow-scan CCDs are well on their way to becoming a standard accessory on new high-end fluorescence microscopes.

CCDs are ideally suited as fluorescence detectors for planar separations such as thin-layer chromatography (TLC) and planar slab electrophoresis. Although the mechanisms of separation for these two methods are different, the end result of both is a separation of a sample (or many samples) onto a two-dimensional medium. Detection of the bands or spots can be accomplished using staining, autoradiography or fluorescence derivatization. Previously, quantitation from the stained or labeled media was performed by scanning densitometry or film imaging followed by scanning. Using a CCD to detect fluorescently labeled bands is an obvious extension due to their success in other fluorescence imaging applications. In some of the original work using scientific slow-scan CCDs, Jackson et al.[71] reported the first visualization of fluorescently labeled proteins in a two-dimensional polyacrylamide gel illuminated with a 150-W tungsten source. Since that time, other researchers have refined the methods for fluorescence detection in slabs[72-75] and in TLC plates.[76] Because the sensitivity, detection limits, and acquisi-

tion speed are all greatly increased using CCD detection, their use should expand rapidly for this application.

B. Raman

One of the areas of spectroscopy that puts the most stringent demands on a detector system is Raman spectroscopy. Typically, less than one in 10^8 of the incident photons undergo Raman scattering, so both an intense monchromatic source and a very sensitive spectrometer are required. To overcome the inherent low sensitivity of the Raman process, most experiments are performed at the limit of available technology. For this reason, CCD array detectors represent an important advance for Raman spectroscopy.[77,78] The detector characteristics already discussed — high QE, low dark current, and large format — all have impact on the use of CCDs for Raman. Richard McCreery has written an excellent discussion on the application of CCDs to Raman spectroscopy.[77]

In the majority of applications of CCDs as Raman detectors, two-dimensional devices are used, but the device is operated as an effective linear array by binning the slit information (either on-chip or in software). Because most commercial CCDs are less than 1024 by 1024 elements, this results in a less than 1024-element spectrum. Although the second dimension of the CCD is rarely used for an analytical measurement, it facilitates alignment of the CCD and spectrograph, allows multiple spectra to be obtained simultaneously by splitting the slit into two or more regions, and enhances the ability to remove high-energy background events by using the redundant slit information.

The first applications of Raman spectroscopy with CCD detection involved looking at the Raman signal from molecules adsorbed onto a surface; because the expected signal under typical conditions is approximately 1 photoelectron per second,[79] low noise, high QE detectors are critical. Murray and Dierker published Raman spectra from monolayer films of cadmium stearate on a silica surface obtained using a CCD.[80-82] Campion compared a scientific CCD and an intensified PDA for examining silicon surfaces with various adsorbed monolayers,[78] and found that the CCD had an improved SNR because of the higher QE of the CCD and taller detector element size compared to PDAs (he used the CCD in a highly binned mode). Another important advantage of a nonintensified system is that the extreme geometrical stability allows spectral subtraction and highly reproducible wavenumber results.

A much higher background is observed for a liquid sample than for thin films. In these cases, background scatter is almost always the dominant noise source, and so detector noise becomes much less important. Both Pemberton and Sobocinski[83,84] and McCreery and co-workers[85,86] have demonstrated the sensitivity and performance obtainable using CCD detection for solution Raman. For example, Figure 13 shows Raman spectra of $(NH_4)SO_4$ in water at several concentrations; the CCD detection system had higher SNR than both PMT- and IS-PDA-based systems.[85,86] Figure 14 shows the arrangement of one such system; this instrument is designed to use a fiber optic sampling head, which greatly simplifies operation be-

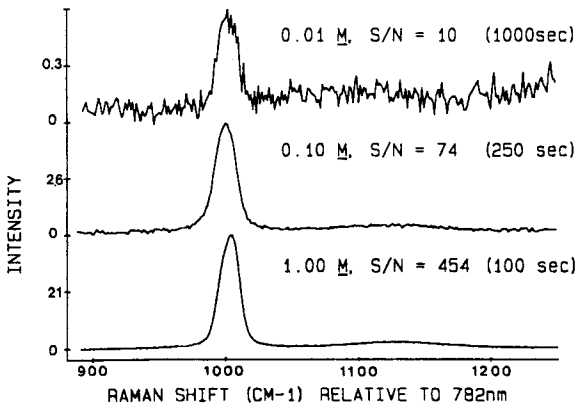

FIGURE 13. CCD Raman spectra of $(NH_4)SO_4$ in water obtained with a 782-nm diode laser. (Reprinted from Wang, Y.; McCreery, R., *Anal. Chem.* **1989**, *62*, 2647. With permission.)

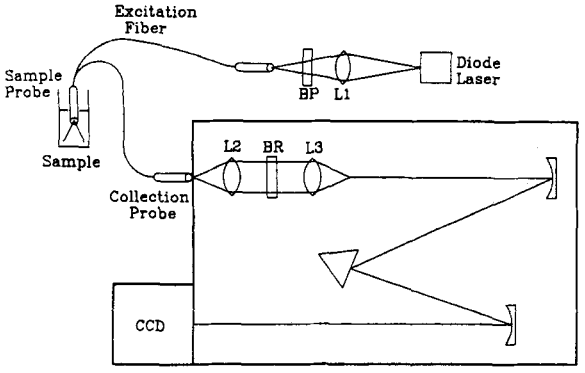

FIGURE 14. An integrated Raman system that uses a diode laser/fiber optics and CCD detection. See Reference 87 for details of the optical system and probe design. (Reprinted from Newman, C.D.; Bret, G.G.; McCreery, R.L., *Appl. Spectrosc.* **1992**, *46*, 262. With permission.)

cause only the fiber tip need be inserted into the sample.[87]

In Raman spectroscopy, it is desirable to cover the spectral region comprising shifts from near 0 to 3000 cm^{-1} with between 1 and 3 cm^{-1} resolution.[88] Unfortunately, sufficient wavenumber coverage or resolution is not possible with readily available CCDs. The standard approach to solving this problem is to take several spectral segments, each of a section of the desired wavelength shift range, and piece them together.[89,90] This increases the measurement time, and because grating drives are not perfect, introduces a small amount of inaccuracy in the wavelength axis. Discontinuities are usually observed at the individual spectral boundaries due to throughput variations as a function of diffraction angle of the grating. An improved approach has been described by Bilhorn, in which the CCD is read using the TDI mode by synchronizing the readout to the scanning of the monochromator.[33,36] This method has the advantages of multichannel detection combined with the flexibility of single channel scanning systems. By synchronizing the shifting of charge in the CCD to the rate that the image moves across the CCD elements, the restrictions placed on wavelength coverage and resolution are relaxed. This method avoids the problems associated with the variations in throughput as a function of diffraction angle. Each element in the spectrum is continuously integrated as it passes through all of the angles that are intercepted by the CCD, thus averaging out any effects associated with angle.

Pelletier has demonstrated another approach based on a low resolution echelle system.[91,92] In this approach, an echelle grating is used that has a high dispersion but highly overlapping orders. A second cross-dispersive element is used to separate the orders. The focal plane of the CCD sees a series of spectral segments that can be thought of as taking the original high resolution Raman spectrum, cutting it into segments, and stacking them on top of each other. Using such as system, a 5000-cm^{-1} range can be covered with 2-cm^{-1} resolution using a 512 by 512 CCD. Because the slit height must be reduced (to accommodate the multiple spectral regions on the CCD focal plane), the system is slightly less sensitive than a conventional CCD Raman system used with a single exposure. If a wide spectral range is required, the two approaches will yield similar SNR, with the echelle having a higher wavenumber reproducibility because of the lack of moving parts.

CCDs have allowed great increases in the sensitivity obtainable in the near-IR region. Because photocathode materials tend to have very poor QEs in this region, the near-IR region has not been highly used with PMT detection. For many important samples, it is not the weakness of the Raman scattering that limits a measurement but the interference of other luminescent materials in the sample. Thus, the reduction of the Raman scattering (because of the υ^4 dependence on cross section) is more than compensated by the reduction in background. Several groups have explored the use of a HeNe laser (632.8 nm),[83] and diode lasers at 782 and 830 nm[82,86,93-95] for Raman experiments. The sensitivity of this approach is limited by the rapidly falling red QE of silicon detectors (see Figure 4). Several deep-depletion CCDs have been fabricated to improve the near-IR performance.[96,97] As non-silicon detectors become available, infrared Raman is expected to become more common.

The ability to combine imaging and Raman is important when looking at heterogenous samples. In fact, a Raman microprobe system has been available commercially for a number of years. However, in these systems, the laser is focused through a microscope objective and rastered across the sample (and the Raman is collected by the same objective). The two-dimensional CCD allows significant improvements to such a system. The straightforward approach is to combine a microscope and a CCD camera (such a system has been introduced by Renishaw Transducer Systems).[98] The sample is illuminated by a laser, the scattered light is collected by an objective, passed through a narrow band pass filter to transmit only a limited Raman shift range, and then imaged onto the CCD. In this approach, only a single wavelength (Raman shift) can be observed at a time. By changing filters, a series of images can be acquired at the desired Raman shifts. A second approach to acquiring the data is to focus the laser into a line, and scan the line across the sample.[99] As the line is focused onto a spectrograph slit, Raman spectra are obtained at each position along the line. As the line is scanned across the sample, the wavelength and X-Y information are acquired. Treado and Morris[100-102] have presented a third approach designed to work with highly photo-unstable compounds; in their system, the laser beam is not used to define the spatial resolution of the sample. Instead, the scattered light from the sample is collected using a microscope and passed through a one-dimensional Hadamard mask, and then onto a spectrograph slit. The mask multiplexes one of the imaging dimensions in time. After all data manipulations, the end result is a four-dimensional data set of intensity versus wavelength, X and Y positions of the sample.

The research previously cited coupled with less expensive CCD detectors, near-IR lasers, and improved imaging spectrographs has attracted commercial vendors. In the last several years, companies such as SPEX, Instruments SA, and Chromex have introduced CCD attachments to several of their spectrometers. Because many of these systems include high efficiency, aberration corrected single-stage spectrometers, holographic laser rejection filters, and CCD detectors, their performance can be excellent. Because of the match of CCD characteristics, the requirements of Raman and the commercial availability of systems from a number of vendors, I expect a large fraction of the new Raman systems sold to use spectrographs equipped with CCD detectors.

C. Molecular Absorbance

Although the reasons to use a CCD for a Raman or luminescence measurement are obvious in terms of the extreme low-light sensitivity offered by these detectors, the driving force behind applying CCDs to ultraviolet/visible (UV/vis) absorbance measurements is less obvious. In an absorbance measurement, one is measuring the difference between two large signals; in an ideal case, one is limited by the shot noise in these measurements (or in many realistic cases, one is limited by source fluctuation noise). Assuming that photon shot noise is the dominant source of noise, then the minimum detectable absorbance signal obtainable from a single read depends only on the full-well capacity of the detector:[21]

$$A_{\min} = -\log\left(1 - \sqrt{8/Q_{\text{sat}}}\right)$$

where Q_{sat} is the full-well capacity of the detector element. For a single read, the minimum detectable absorbance occurs just before detector saturation. A CCD with a full-well capacity of 300,000 e can measure the absorbance of a sample with an uncertainty no better than 0.002 absorbance units; of course, as multiple reads are added in computer memory, the minimum detectable signal is improved. For a further discussion of the limiting SNR obtainable using an integrating detector for absorbance, see the discussion in Bilhorn et al.[21] Because low read noise and insignificant dark current are not

as important for such measurements as large full-well capacity and the ability to read the device quickly, linear PDAs work well for acquiring UV/vis absorption spectra.

Although there are no reports of using CIDs for UV/vis measurements, they are well suited because of their high full-well capacity and the nondestructive readout mode. For a CCD or a PDA system used at the focal plane of a spectrometer, the array readout rate must be shorter than the time it takes to saturate any detector element (the readout rate is determined by the wavelength region with the highest photon flux). Many commercial PDA systems use a deuterium lamp and cover the 200- to 600-nm range. Although the readout rate is dependent on the flux falling at the detector in the ultraviolet region, the energy in the 500- to 600-nm region is typically more than an order of magnitude lower. At these longer wavelengths, the readout rate is far from optimum. Unlike the PDA or CCD, the readout for a CID can be optimized for each wavelength interval by reading each detector as it approaches saturation; this allows the maximum SNR to be obtained at the minimum data acquisition rate.

Even though not commonly used, the two-dimensional format of a CCD allows high quality absorption measurements to be made when two-dimensional (i.e., spatial) information is required in such applications as bright-field microscopy, measuring heterogeneous samples or the absorbance from analytes separated using TLC plates or electrophoresis gels. As one example, absorbance measurements of highly absorbing films can be confounded by the presence of small pinholes and, in some cases, by large variations of absorbance across the sample.[18] A prototype absorbance system used the CCD as a detector in an imaging spectrometer and spatially measured the absorbance of optically thick films. The areas containing film defects (pinholes) were detected and the uniform areas of the film were used to calculate the absorbance of the sample. In this system, absorbances as high as 5 absorbance units were easily measured while discriminating against the pinholes; without removing the "stray light" from the pinholes, the resulting spectra would be seriously distorted.

As mentioned in the previous discussion of molecular fluorescence detection, CCDs are well suited to imaging TLC plates and electrophoresis gels because the two-dimensional format of the detector is required.[76] Although low-noise CCD systems are not required for absorbance measurements, high precision digitization is required. Cosgrove and Bilhorn[103] have demonstrated the use of a cooled CCD for absorbance imaging of TLC plates and found that the peak shape and sensitivity were similar to those obtained with a mechanical slit scanning densitometer with a considerable saving in measurement time and a large improvement in the day to day precision. CCDs also have been used as detectors in slab electrophoresis.[72,73] As one example, Yeung and co-workers[104] have developed a system for on-line detection of DNA using the absorbance of 254-nm light. The CCD system allows on-line monitoring of the separation. With a detection limit of approximately 5 ng/band, the CCD system has a better detectability than other on-line methods, but approximately five times less sensitivity than the ethidium bromide method. Of course, no staining or destaining is required to recover the DNA as with the more common ethidium bromide staining. As in the TLC experiments, one of the most important steps in using a CCD as a detector in an electrophoresis experiment is obtaining an accurate reference exposure to correct for variations and inhomogeneities in illumination or in the gel. In many cases, the quality of the flat field exposure determines the minimum amount of material that can be detected.

The CCD is starting to replace photographic film as a detector in many TLC and electrophoresis applications. Not only are the detection limits better, but the quantitative nature of the information gained from a CCD is a large advantage. A commercial electrophoresis scanning system is already available from Millipore, and as the price of such

systems becomes reasonable, CCD detection of slabs and plates should become routine.

D. Atomic Spectroscopy

Atomic emission spectroscopy (AES) is the most common analytical method for trace elemental analysis. The large number of resolution elements, sensitivity, and dynamic range of available CTDs have allowed significant improvements to be made in AES system performance. However, because AES can require a seven order of magnitude dynamic range and more than 100,000 spectral resolution elements, the application of a CTD is not straightforward. In what follows, an overview of the applications of CTDs to analytical AES is presented. Thermo Jarrell Ash has introduced a commercial system, and recent conference talks indicate that Perkin Elmer and Baird will soon follow.

Traditionally, AES is performed with a slew-scan instrument or a direct reader. Since the 1970s, numerous groups have attempted to overcome problems with these approaches using a variety of array detectors.[105-108] However, until the advent of CTDs, one could either have the sensitivity and dynamic range of the PMT, the high resolution simultaneous detection offered by photographic emulsion, or a much lower resolution and much less sensitive (than the PMT) detector array. To cover the UV to the near-IR wavelength region with the resolution required for atomic spectroscopy (i.e., < 0.01 nm), several hundred thousand resolution elements are optimum. Obviously, linear arrays are not available with the number of elements required and so the only practical alternative is the echelle spectrometer. An echelle system employs two dispersive elements: the echelle grating as a high dispersion element, and a low dispersion element oriented so that its direction of dispersion is at a right angle to the echelle grating.[109] As shown in Figure 15, the resulting output is a focal plane image that looks like a series of spectra arranged as text on a page, each line consisting of a contiguous piece of the whole spectrum. The

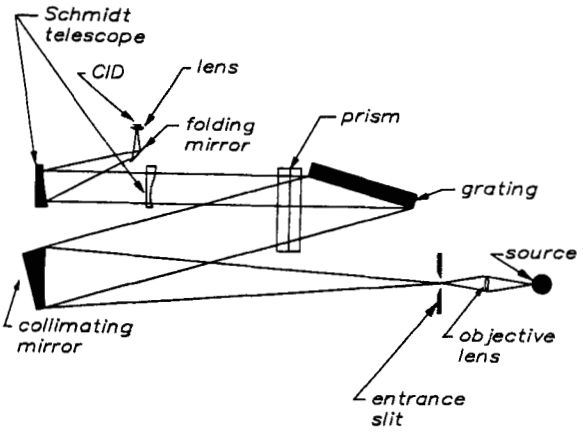

FIGURE 15. The spectrometer optical diagram for the University of Arizona CID17 echelle plasma emission system. The echelle spectrometer produces a focal plane image compatible with the 6.5- by 8.7-mm size of the CID17. (Reprinted from Bilhorn, R.B.; Denton, M.B., *Appl. Spectrosc.* **1989**, *43*, 1. With permission.)

spectrometers designed to use a CTD are similar to those designed to use a photographic emulsion except the image size is greatly reduced in order to produce an echellogram comparable in size with the silicon detectors.[17,18,21,43-45,110]

Several generations of CTD/echelle system have been explored at the University of Arizona.[17,18,21,43-45,47] The design of a later system is shown in Figure 15. A quartz cross dispersive element is used and the image reduction is achieved by using a short focal length camera mirror.[47] The focal plane of the echelle sees many molecular bands and atomic lines from the solvent and a bright argon plasma background. Superimposed on this can be thousands of emission lines from the sample. Figure 16 shows raw and background subtracted CCD echellograms from a mixture of Ni, Pb, Cr, Mn, Ca, and Fe.[37]

Although Figure 16 shows echellograms obtained with a CCD, this system has been extensively characterized using a CID17 detector. With this detector, the system obtains a 0.005-nm/pixel resolution at 300 nm and a spectral range from 200 to 550 nm. The CID architecture offers several advantages for AES; notably, resistance to blooming and the random access readout mode described pre-

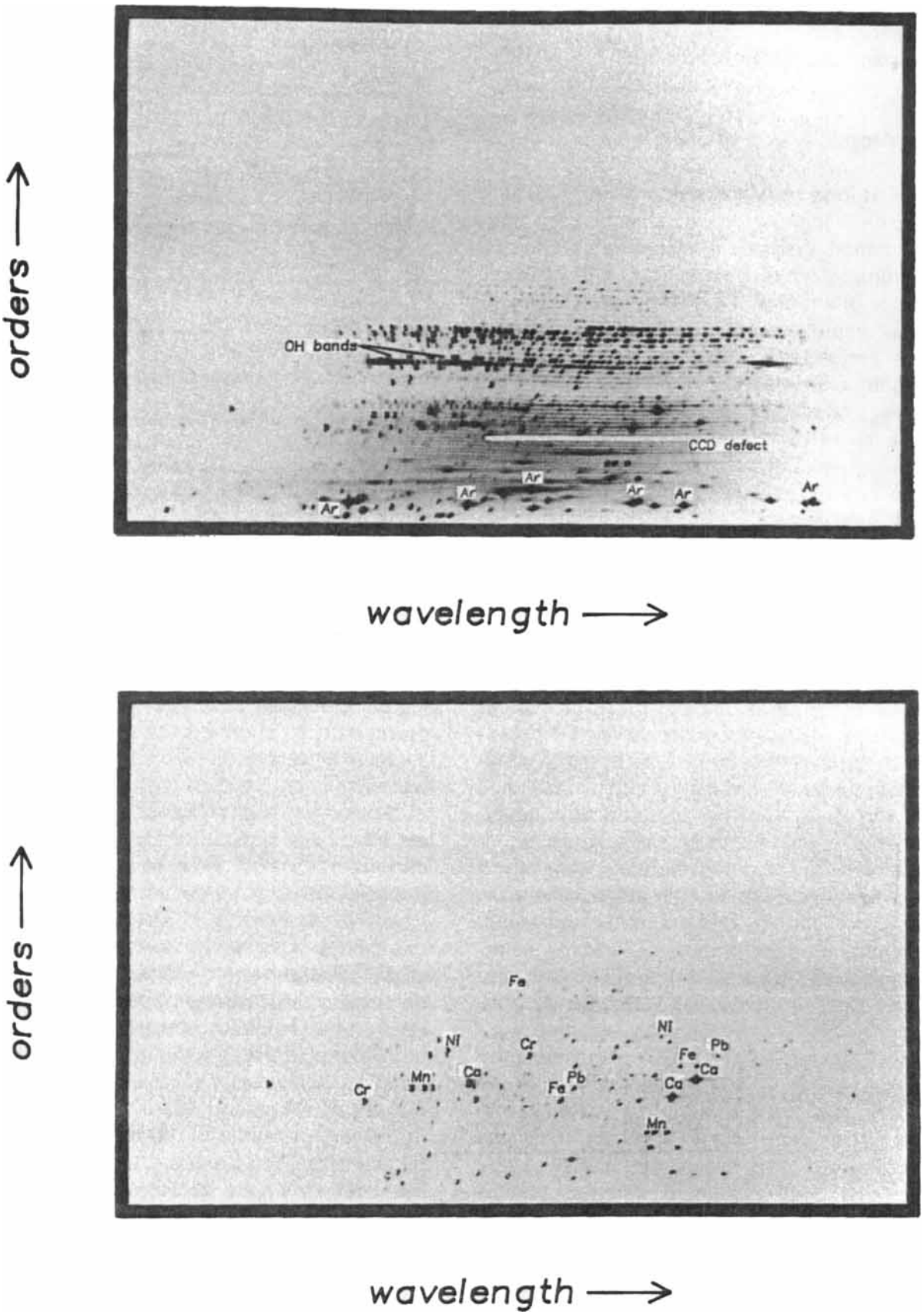

FIGURE 16. The raw and background subtracted echellograms of a six element mix obtained using a 3-s exposure of the CTD to a direct current plasma and the optical system illustrated in Figure 15. (Reprinted from Sweedler, J.V.; Jalkian, R.D.; Pomeroy, R.S.; Denton, M.B., *Spectrochim. Acta* **1989**, *44B*, 683. With permission.)

viously. Although full frame reads are possible, the CID is capable of an expanded dynamic range by interrogating those portions of the CID that contain emission lines for the elements of interest and recording the intensity information for each line just prior to saturation. Because the CID is not subject to charge blooming, faint emission lines can be determined long after intense lines have saturated. To improve precision and accuracy, the spectral region adjacent to each line is also read and a background corrected intensity is calculated.[45] Because an echelle system has no moving parts and records the background for the identical observation period as the analytical line, high quality background corrections are possible.[45] The benefits of CTD detection from transient AES sources such as arcs and sparks also have been demonstrated using the University of Arizona echelle system.[110] The ability to combine the best features of photographic film with the precision of CTD detection allows both qualitative and quantitative analysis to be performed using direct solid sampling of a spark source.

Thermo Jarrell Ash has introduced a commercial system that also uses a CID17 as the detector.[48] Their echelle system covers the range from 170 to 800 nm with a greater light collection efficiency than the University of Arizona system, but with a reduced resolution (at best, 0.02 nm/pixel). The spectrometer and detector performance have been described in detail by Pilon and co-workers[48] using an inductively coupled plasma source.

CCDs also have been investigated for AES. CCDs offer the advantages of lower read noise and larger formats, but obviously they do not allow the nondestructive readout mode and many CCDs suffer from charge blooming. A comparison of an RCA CCD and a CID17 on the University of Arizona echelle system has been published.[37] Charge blooming limits the ability to detect trace components in the presence of complex matrices. This report also presented preliminary data on the use of an antiblooming CCD for AES. With such a system, a series of exposures can be used to increase the dynamic range of the detector with little increase in total observation time.[37] For example, if a series of three exposures of the plasma are taken with a CCD using observation times of 0.5, 10, and 200 s compared to a single 200-s exposure with a CID, the total analysis time is not significantly different between the two approaches (neglecting the array readout time, which can be significant in CCDs).

Several additional investigators have designed custom CCD/echelle instruments, with notable systems described by Scheeline et al.,[111] Bilhorn,[112] and Krupa et al. (Baird Corporation).[113] The system developed by Bilhorn uses an antiblooming Kodak KAF1300L CCD that has a 1280 by 1024 element format. Bilhorn measured that the antiblooming drains on this CCD can conduct away $\approx 5 \times 10^6$ e/s, and so these antiblooming CCDs can be used in AES.[112] The advantages associated with the greater CCD array size are obvious because the spectrometer covers the wavelength range from $\approx$ 180 to 800 nm with a resolution of 0.0025 nm/pixel at 300 nm.

Perhaps pointing to the future of CTD design, Perkin-Elmer has taken a completely novel approach to a CTD-based AES system.[114-116] They have developed a custom CCD consisting of hundreds of small CCD subarrays located on a large silicon substrate with each subarray located at the positions that the major emission lines should fall on their echelle focal plane. Because each subarray can be accessed separately, different integration times are possible for each subarray. Although charge blooming is a possibility within each subarray, the bloomed charge cannot migrate to other subarrays and so the device is effectively antiblooming. These linear CCD subarrays have a high QE because they use less overlying gate structure and maintain high CTE by using a series of ion implants. The block diagram of this instrument, the Optima 3000, is illustrated in Figure 17. The optical system divides the emission into two wavelength regions: a visible region from 380 to 860 nm and the ultraviolet region from 160 to 380 nm. Overall, this system overcomes the limited size of CID detectors and limitations of CCD full frame readout. The system acquires spectra

with a resolution of 0.0025 nm/pixel and mimics the RAI readout mode. Although there are only several hundred CCD subarrays on the detector, multiple lines fall on many subarrays and so several thousand emission lines can be monitored,[115] which is similar in number to the University of Arizona and Thermo Jarrell Ash systems described previously. Although this system requires a carefully designed and aligned optical system, it overcomes the shortcomings of commercially available CTD technology. The Perkin-Elmer approach is notable because it demonstrates what can be done by redesigning a CTD for a particular chemical analysis application.

In the molecular fluorescence and Raman work described previously, the type of information acquired with the CTD is similar to that available with previous technologies; however a CTD/echelle system allows data processing never before possible. Because the entire emission spectrum is acquired with a single exposure, qualitative and semiquantitative surveys for a large number of elements are straightforward. As one example, Pomeroy and co-workers[117] demonstrated the analysis of a ~20-μg particulate material found in a filter in the Respiratory Care Unit of the University of Arizona Medical Center. In this type of analysis, the limited sample is aspirated into a direct current plasma, a single echellogram is taken, and then at the analyst's leisure, the stored echellogram can be checked for the presence of any desired element. Pomeroy et al. also studied the amount of sample required to obtain quantitative results from SRM 1633a, coal fly ash, using a single 2-min exposure; their results are summarized in Table 2.[117]

Because these systems have no moving parts and have excellent stability, calibration information for a number of elements is easy to obtain. The flexibility afforded by such systems in terms of wavelength selection is an important feature compared to conventional scanning or polychromator systems. The choice of spectral lines to be used can be custom tailored to the components of the sample being measured. For example, the most intense lines are selected for trace components and less intense lines are used for

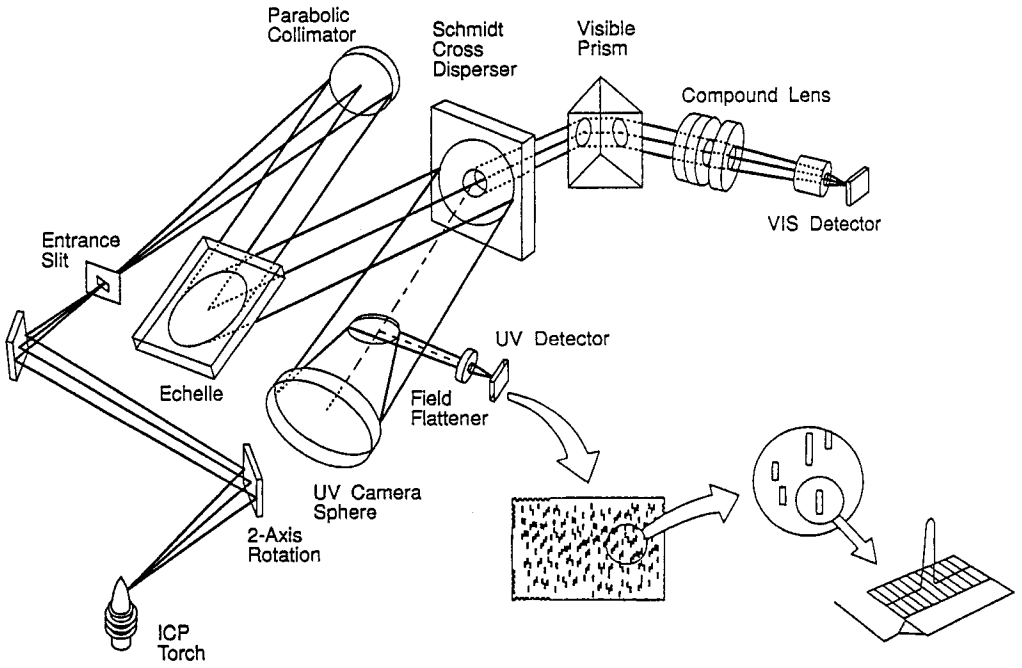

FIGURE 17. Spectrometer optical diagram for the Perkin Elmer Optima 3000 system. The insert shows the unique multiple subarray CCD. Copyright 1993 by the Perkin-Elmer Corporation.

elements at high concentrations in order to avoid problems with self-absorption. Multiple lines are available for each element to enhance precision, and known spectral interferences can be avoided in cases that alternative spectral lines are available. Because the echellogram has emission lines from the sample, the sample matrix and information about the source and excitation process, a number of diagnostic tests become possible on source and nebulizer performance during the actual analyses,[118] enabling powerful expert systems to be implemented.[119] Barnard of Perkin-Elmer reports[116] that their system obtains linear working curves for most elements at concentrations an order of magnitude lower than the source and nebulizer fluctuation noise limit. By monitoring the appropriate emission lines and correcting all results as needed, almost every analysis can become background shot-noise-limited. Not surprisingly, the software development for a commercial AES/CTD system is the largest cost associated with the instrumentation.

While much progress has been made using CTDs for atomic emission, relatively little has been demonstrated with atomic absorption. Ideally, a resolution of greater than 0.001 nm/pixel is desired for continuum source atomic absorption. The microsampling furnace techniques available for atomic absorption spectroscopy hold great promise as a powerful analytical tool for trace element analysis when sample sizes are limited.

As one of the few studies yet published, Pardue and co-workers[120] described a system using a commercially available CID camera, a modified echelle system, and a xenon arc lamp source. The CID camera was used as supplied and was operated at room temperature and, thus, the CID detector did not support the NDRO or RAI readout modes. To provide adequate wavelength resolution with the limited number of elements available, a limited ($\approx$ 40-nm) spectral window was observed. Even these preliminary results demonstrate the ability to perform multielement analyses, increase the dynamic range and improve precision by using multiple lines. Harnly has published several studies[121,122] describing the use of diode detection for graphite furnace continuum source AA, and

TABLE 2
Analysis of SRM 1633a Coal Fly Ash

Element	NBS certified value	Coal fly ash concentation in solution		
		A	B	C
Al	140[a]	139 ± 7	130.5 ± 6	132 ± 8
Ba	1.50[a]	1.53 ± 0.04	1.55 ± 0.07	1.50 ± 0.3
Cd	0.001 ± 0.002	0.001 ± 0.0003	—	—
Ca	11.1 ± 0.1	10.80 ± 0.02	11.1 ± 0.2	10.8 ± 0.5
Cr	0.196 ± 0.006	0.190 ± 0.01	0.18 ± 0.03	—
Cu	0.118 ± 0.003	0.13 ± 0.01	0.13 ± 0.03	—
Fe	94 ± 1	93.7 ± 0.5	95 ± 3	98 ± 5
Pb	0.072 ± 0.004	0.070 ± 0.004	0.08 ± 0.02	—
Mg	4.6 ± 0.1	4.61 ± 0.05	5.3 ± 0.3	5 ± 3
Mn	0.19[a]	0.18 ± 0.02	0.18 ± 0.03	—
Ni	0.127 ± 0.004	0.13 ± 0.01	0.150 ± 0.05	—
Si	228 ± 8	231 ± 3	230 ± 10	250 ± 30
Sr	0.83 ± 0.03	0.84 ± 0.01	0.87 ± 0.05	0.50 ± 0.5
Ti	8.0[a]	9.40 ± 0.70	8 ± 1	5.00 ± 3
V	0.30[a]	0.311 ± 0.009	0.29 ± 0.02	—
Zn	0.22 ± 0.01	0.240 ± 0.03	0.23 ± 0.03	—

Note: All values in micrograms per gram. A has a coal fly ash concentration of 1000 μg/ml, B has 400 μg/ml, and C has 40 μg/ml.

[a] Noncertified value.

has developed the equations describing the advantages of such a system. He recently presented preliminary results[123] using a scientific CID for continuum source AA that further demonstrates the advantages of a high resolution two-dimensional detector for this application.

In addition to using the CTD at the focal plane of an echelle, two-dimensional detectors have been used in a number of diagnostic studies of atomic sources. CCDs can be used for low resolution spectral and one-dimensional spatial imaging, two-dimensional wavelength resolved imaging, or in time-resolved applications. Figure 18 shows a low resolution atomic emission spectrum of a slice of a spark obtained from a sample of cold rolled steel.[124] In addition, the CCD can be located at the exit of a two-dimensional imaging monochromator.[125] Hieftje et al.[125,126] have developed a wavelength-resolved tomographic imaging system to image the distribution of various atomic species in plasmas. Another application involves using one of the CCD dimensions to store information acquired at different times;[127,128] Mork and Scheeline[127] developed such a system to follow the evolution of spark plumes with a microsecond resolution. The multidimensional information obtainable using CTDs allows much more information-rich diagnostic studies of atomic sources and should lead to improved atomic emission sources.

E. High-Energy Photons and Particles

During the last 10 years, there has been a considerable effort to use CCD detectors for imaging a number of types of radiation in addition to visible and near-visible photons in the fields of astronomy and astrophysics,[129-131] biology,[132] and chemistry.[133] This section briefly reviews the trends in the detection of X-rays and high-energy particles

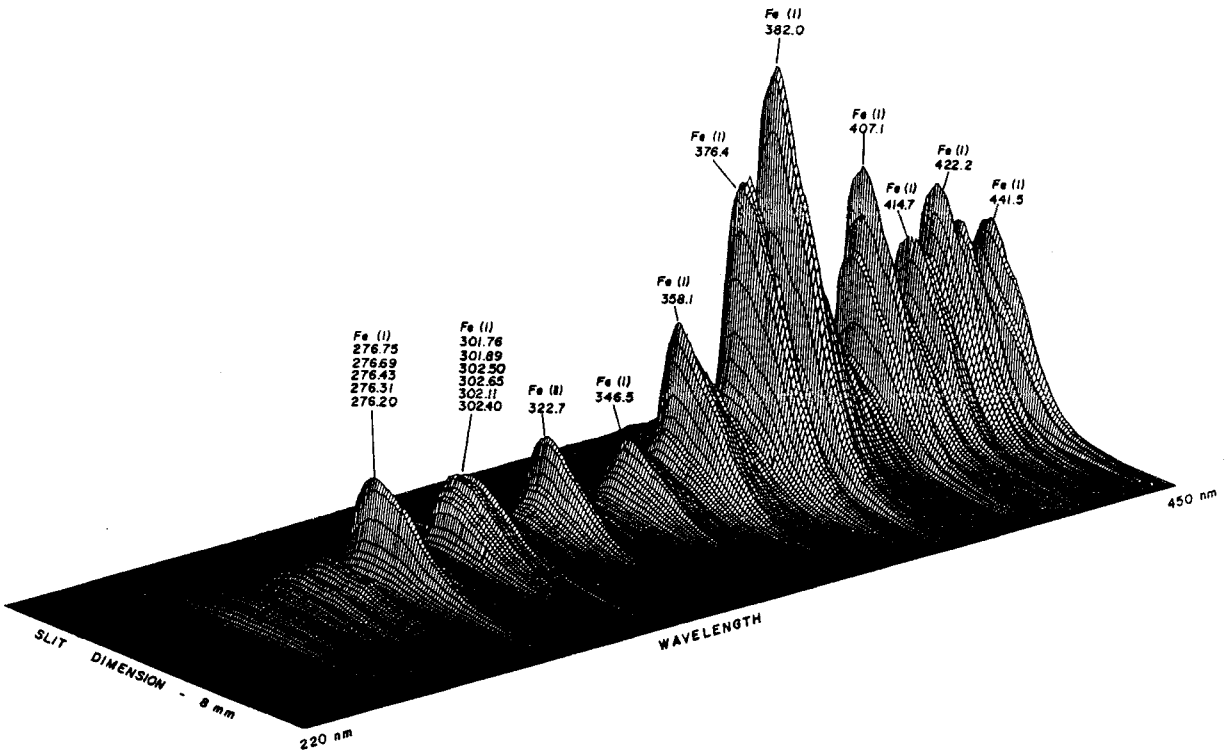

FIGURE 18. Wavelength-resolved spectral image from a single unidirectional spark from a sample of cold rolled steel. (Reprinted from Kolczynski, J.D.; Pomeroy, R.S.; Jalkian, R.D.; Denton, M.B., *Appl. Spectrosc.* **1989**, *43*, 887. With permission.)

using CCDs. Such detection is often accomplished by converting the high-energy events into low-energy visible photons by using a phosphor screen.[133-135] Such indirect detection methods can work well and provide high spatial information. Because the image of the screen can be optically magnified to fit the dimensions of the CCD, considerable flexibility exists in matching the imaging requirements to the CCD.

In the following text, the *direct* imaging of low-energy X-rays and particles using a CCD is described. From the late 1970s, the potential for CCDs to directly detect single X-ray photons has been explored.[136,137] In the visible spectral region, a single photon produces a single electron–hole pair (e–h) pair, whereas for X-ray photons, hundreds of e–h pairs can be created with the number of e–h pairs created dependent on the photon energy. Quite early in the development of CCDs, it was realized that a CCD can be used for energy-resolved X-ray imaging, in which the CCD can simultaneously count X-ray photons *and* estimate their energy.[138] Thus, under optimum conditions, it is possible to use an area CCD to determine three-dimensional information (intensity information as a function of X, Y, and energy). Over the last 10 years, Janesick and co-workers have investigated the detector requirements to achieve optimum performance from a CCD for direct X-ray detection.[139,140]

What limits the energy resolution obtainable with a CCD? On the average, it takes 3.65 eV of energy to produce a single e–h pair in silicon; thus a Mg $K\alpha$ photon, with an energy of 5.9 keV, should produce 1620 e. However, there is a statistical variation in the amount of charge generated because a finite amount of energy is distributed into the silicon lattice by non-e–h processes. This uncertainty was first described by Fano in 1947,[141] and reflects the ultimate limit of detector energy resolution possible:[140]

$$\mathrm{FWHM} = 2.356\sqrt{E/36.5}$$

where the full width at half maximum (FWHM) of the peak has units of electrons, and E is the photon energy in electron volts. For the Mn $K\alpha$ photon of 5.9 keV, the theoretical energy resolution is approximately 110 eV or 30 e. This is the best that can be done if the CCD read noise is insignificant and the CTE is unity. To remain limited by the uncertainty first described by Fano (Fano noise limited) over the soft X-ray region, the read noise of the CCD must be kept below 2 e rms (root mean square) and the CTE must be extremely close to unity.[140] Currently, energy dispersive X-ray imaging places the most stringent requirements on CCD performance of any application. Remarkably, Janesick has reported the development of several CCDs that reach these levels.[23,140] Such an energy dispersive X-ray spectrum is shown in Figure 19 for an ^{55}Fe source. Although other researchers have not demonstrated the same level of energy resolution, Lumb[142] and Clarke[143] have also described such systems for X-ray spectrometry.

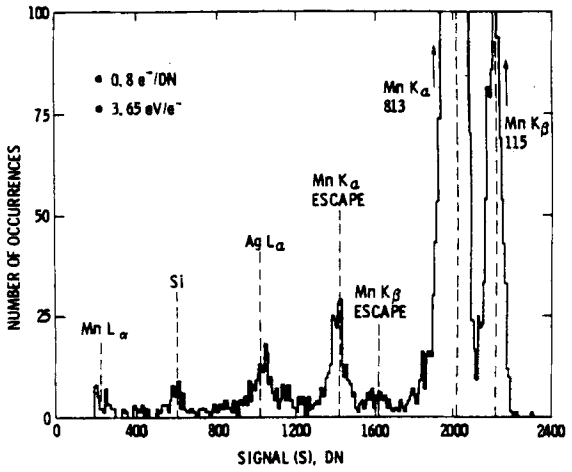

FIGURE 19. X-ray spectrum of an ^{55}Fe source using a CCD in an energy-dispersive mode. The Mn K_α and the Mn K_β peaks, both escape peaks, and the silicon absorption peak are shown. (Reprinted from Epperson, P.M.; Sweedler, J.V.; Bilhorn, R.S.; Sims, G.R.; Denton, M.B., *Anal. Chem.* **1988**, *63*, 327A. With permission.)

A significant source of nonideal behavior in energy dispersive X-ray spectrometry is that not all the charge from a single X-ray event is collected by a single detector. In many cases, the photogenerated charge is split between two adjacent detectors. This splitting of the charge packet can be greatly reduced with properly designed overlying electrode geometry (i.e., improved CCD de-

sign) and its effects can be minimized with the development of the appropriate software that looks for such events and determines the total charge of the split event. Another limitation of using a CCD in such an energy dispersive mode is high flux rates. If the flux rate is high enough that multiple events become likely, it becomes problematic to resolve a multiple event from a single, higher energy event. This restriction on maximum flux rate depends on CCD readout rate, so as faster readout rates become available, higher flux observations become possible.

In addition to X-rays, CCDs have been used for the direct detection of beta particles,[144] heavy quarks,[145] and other high-energy particles. The ability to detect ionizing radiation with good spatial resolution has been the driving force behind the research. One limitation of directly detecting X-rays and high-energy particles is that if they possess sufficient energy, they will damage the silicon lattice or cause significant degradation of CCD performance over time. This is the reason that CCDs are normally used to detect X-rays of < 30 keV and low-energy particles. In fact, although much of the early development work on CCDs has been funded by NASA with the goal of using them on interplanetary missions, their susceptibility to damage from long-term exposure to ionizing radiation has hampered their use on these missions. As the details of using CCDs for the direct detection of X-rays and high-energy particles are perfected and the newest generation of low-noise CCDs become common, an increase in the use of these detectors in such applications will occur. As the price of these detectors drops, they may even be used in applications where the energy of the photon or particles is high enough to require replacing the detector on a regular basis.

V. CONCLUSIONS

The goals of this review have been twofold. The first is to describe the operation and characteristics of CCD and CID detectors, with particular attention given to those performance specifications that have the greatest impact on their use in chemical analysis. Perhaps one of the most surprising aspects in the evolution of the CCD is that their performance specifications have continued to improve. PMTs have always been limited by their poor QE and PDAs have been limited by the large read noise inherent in their readout process; these characteristics have not been significantly improved. On the other hand, users of CCDs a decade ago considered a 50-e read noise and a 40% peak QE excellent. Today, the same purchaser of a CCD expects a read noise of under 5 e, a peak QE in excess of 80%, and a dark current for a properly cooled device of 1 e/h per detector. Although not commonly used, several manufacturers already are placing skipper amplifiers on their devices that can provide a read noise of < 1 e with multiple nondestructive reads. Devices have been reported with no measurable charge transfer losses, greatly improved read rates, a responsivity from the near-infrared red region to the soft X-ray region, formats as large as 16 million detector elements and very few cosmetic defects. As such characteristics become more common, imaging detectors are finally becoming available with almost the theoretical limit of detector performance.

The second objective has been to review the status of CCDs and CIDs in the field of chemical analysis. Although the application of CTDs to the major areas of chemical analysis have been described, CTDs have also been used as detectors in other areas such as circular dichroism.[146] Many of the CTD/spectrometer and imaging systems offer greatly improved sensitivity, spatial resolution and/or time resolution compared to single channel or previous array systems. Although many of the optical systems outlined have been described in context to a specific area such as Raman or atomic spectrometry, most of the hardware implementations can be used in other applications. The acceptance of these detectors has been most rapid in those areas which already use two-dimensional detection schemes such as microscopic imaging. CCDs are now com-

monly used for Raman and fluorescence detection because these detectors allow experiments that are not feasible using other detection methods. However, the most effective use of two-dimensional array detectors often requires a complete rethinking of the design requirements of the measurement system. Most researchers are not willing to devote the required effort to design, build, and optimize such systems. Thus there is a significant delay between the demonstration of an approach and the commercial availability of the new technology. Over the last two years, several analytical instrumentation companies have started offering complete systems using CTDs in the areas of atomic spectroscopy, fluorescence, and Raman spectroscopy. As this trend continues, CTDs will become common and the performance they bring to chemical analysis will become routine.

ACKNOWLEDGMENTS

The financial support of the National Science Foundation Young Investigator Award (CHE 92-57024), a Henry and Camille Dreyfus Foundation New Faculty Award, a Science and Engineering Fellowship from the David and Lucile Packard Foundation, and of the Whitaker Foundation is gratefully acknowledged.

A GLOSSARY OF CTD TERMINOLOGY

Bias frame. A dark exposure of the CTD that is subtracted from all subsequent exposures. This removes the dark offset and any fixed pattern response of the detector array.

Binning. The combination of the charge from multiple and contiguous detector elements into a single charge packet prior to readout of the charge packet by the on-chip amplifier in a CCD detector.

Blooming. After the charge storage capacity of an individual detector element is exceeded, blooming is the process of excess charge spilling into adjacent detector elements.

Buried Channel. An ion implantation into the p-type region to form a doped n region below the surface of the device. The resulting potential gradient causes the photogenerated charge to be stored away from the surface silicon–silicon oxide interface, greatly reducing dark current and hysteresis effects and improving low level CTE.

Charge-coupled device (CCD). A member of the class of charge-transfer devices in which the photogenerated charge is read by the step-wise transfer of the charge from the imaging area to a readout amplifier.

Charge-injection device (CID). A member of the class of charge-transfer devices in which the photogenerated charge is read by shifting the charge back and forth between two electrodes within each detector element.

Charge-transfer device (CTD). An analog integrated circuit that consists of an array of MOS capacitors. The incident photons are converted to electrons and stored under an electrode. The amount of charge contained in an element is measured by either shifting it within an element (intracell readout, used by CIDs) or shifting it to an on-chip amplifier (intercell readout, used by CCDs).

Charge-transfer efficiency (CTE). A measure of the ability of a CCD to transfer a charge packet intact from the detector element where it is collected to the amplifier. It represents the fraction of charge that makes each transfer. A CTE of 1 indicates no charge-transfer losses.

Crosstalk. For early CIDs, the charge contained in a row of collection electrodes can effect the measurement of charge at other detector elements in that row. However, the effect of the crosstalk can be removed using several corrections. Newer CIDs do not suffer from detectable crosstalk.

Dark current. The charge generated in the absence of illumination. Because the generation rate is temperature dependent, most CTDs are cooled to reduce the dark count rate to extremely low levels.

Flat field. A uniform exposure of the CTD to an illumination source to correct both system (optical) variations and detector nonuniformities to the average response.

Multipinned phase (MPP). A method of biasing the phases in a CCD during the integration process to greatly reduce the dark current at a given temperature. This method also reduces the full-well capacity of the CCD.

Non-destructive readout (NDRO). A method of reading out a CID that allows the charge information to be measured without destroying the charge contained within the element (hence the readout can be repeated).

Output node. The output node is the input to the on-chip amplifier in a CCD and represents the last gate that the charge is transferred to in the CCD.

Pixel. An individual detector element in a CTD.

Phase. In a CCD, this refers to a set of electrodes that are electrically connected together. Thus a three-phase CCD has three sets of overlying electrodes for which the voltage can be independently controlled for each CCD region.

Potential Well. A graphical method used to indicate the "favorableness" of a region for holding the charge carriers. As one example, as an electrode is made more positive, the region under the electrode becomes more energetically favorable to electrons, so a deeper potential well is drawn.

Random access integration (RAI). A readout mode used with a CID where the intensity information in a detector element is read nondestructively, and the 191intensity and time are recorded. Because different regions of the CID can have vastly different exposure times for a single exposure, this allows the effective dynamic range from a single exposure to be greatly increased.

Quantum efficiency. In a silicon CTD, this is defined as the number of electrons collected divided by the number of incident photons (times 100%). Thus, a QE of 90% at 600 nm means 90% of the incident 600-nm photons create an e–h pair and that the electron (or hole) is collected. At wavelengths below 300 nm, the situation becomes more complex because the photon has sufficient energy to create more than one e–h pair. As an example, at 180 nm, a QE of 40% could indicate that 20% of the photons create two e–h pairs, 40% create a single e–h pair, or most likely, that the situation is somewhere between these two limits. The shot noise

and read noise of the detector in terms of minimum detectable numbers of photons is different in each case.

Summing well. A gate at the end of the serial register of the CCD. The charge in the last serial element is transferred to the summing well, where it can then be transferred to the output node. By allowing independent control of the serial register, the transfer of charge into the summing well and the transfer of charge to the output node, the readout noise becomes independent of the serial binning. Relatively few CCDs are equipped with a summing well.

Surface Channel. A CTD without a buried channel. Currently, all CCDs used in scientific applications use a buried channel architecture and all CIDs use surface channel architecture. In a surface channel device, the photogenerated charge is stored near the surface silicon–silicon oxide interface.

Time-delayed integration. A readout mode of the CCD in which the parallel shift rate of the CCD is synchronized to a moving scene. In this way, the image of an object sweeps across the CCD at the same rate that the photogenerated charge is shifted toward the serial register. This results in large increases in sensitivity compared to a linear detector and allows the CCD to acquire long swaths from a moving image.

REFERENCES

1. Mathies, R.A.; Peck, K.; Stryer, L. *Anal. Chem.* **1990**, *62*, 1786.
2. Soper, S.A.; Shera, E.B.; Martin, J.C.; Jett, J.H.; Hahn, J.H.; Nutto, H.L.; Keller, R.A. *Anal. Chem.* **1991**, *63*, 432.
3. Whitten, W.B.; Ramsey, J.M.; Arnold, S.; Bronk, B.V. *Anal. Chem.* **1991**, *63*, 1027.
4. Stevenson, C.L.; Winefordner, J.S. *Appl. Spectrosc.* **1992**, *46*, 407.
5. Sweedler, J.V.; Bilhorn, R.B.; Epperson, P.M.; Sims, G.R.; Denton, M.B. *Anal. Chem.* **1988**, *63*, 242A.
6. Chase, B. Arrays for detection beyond one micron, in *Charge Transfer Device Detectors in Chemistry*; J.V. Sweedler, K.L. Ratzlaff, M.B. Denton, Eds.; VCH: New York, 1993.
7. Dereniak, E.L.; Crowe, O.G. *Optical* Radiation Detectors, Wiley, New York, 1984.
8. McCaughrean, M. *Sky & Telesc.* **1991**, July, 31.
9. DiCicco, D. *Sky & Telesc.* **1991**, March, 257.
10. Eicher, D. *Astronomy* **1991**, Feb., 70.
11. Boyle, W.S.; Smith, G.E. *Bell Syst. Tech. J.* **1970**, *49*, 587.
12. Amilio, G.F.; Thompsett, M.F.; Smith, G.E. *Bell Syst. Tech. J.* **1970**, *49*, 593.
13. Michon, G.J.; Burke, H.K. *Dig. IEEE, Int. Solid State Circuits Conf.* **1973**, *16*, 138.
14. Janesick, J.R.; Elliott, T.S. *History and Advancements of Large Area Scientific CCDs*; Astronomical Society of the Pacific: Tucson, AZ, 1991.
15. Aikens, R.S.; Lynds, C.R.; Nelson, R.E. *Proc. SPIE* **1976**, *78*, 65.
16. Ratzlaff, K.L.; Paul, S.L. *Appl. Spectrosc.* **1979**, *33*, 240.
17. Sims, G.R.; Denton, M.B. Simultaneous multielement emission spectrometry using a charge injection device, in *Multielement Imaging Detectors*; Y. Talmi, Ed.; ACS Symposium Series 236; American Chemical Society: Washington, D.C., 1983; Vol. 2.
18. Epperson, P.M.; Sweedler, J.V. Bilhorn, R.S.; Sims, G.R.; Denton, M.B. *Anal. Chem.* **1988**, *63*, 327A.
19. Janesick, J.R., Elliott, T.S.; Collins, S.; Blouke, M.M.; Freemen J. *Opt. Eng.* **1987**, *26*, 692.
20. Janesick, J.R.; Elliott, T.S.; Daud, T.; Campbell, D. *Proc. SPIE* **1986**, *627*, 543.
21. Bilhorn, R.B.; Epperson, P.M.; Sweedler, J.V.; Denton, M.B. *Appl. Spectrosc.* **1987**, *41*, 1125.
22. Bilhorn, R.B.; Sweedler, J.V.; Epperson, P.M.; Denton, M.B. *Appl. Spectrosc.* **1987**, *41*, 1117.
23. Janesick, J.R. New technologies and remedies under development at JPL to circumvent current performance limits for the scientific CCD, the 2nd Int. Conf. on Scientific Optical Imaging, December 1992, Grand Cayman.
24. Sweedler, J.V.; Jalkian, R.D., Denton, M.D. *Appl. Spectrosc.* **1989**, *41*, 953.
25. Epperson, P.M.; Sweedler, J.V.; Denton, M.B.; McCurnin, W.; Aikens, R.S. *Opt. Eng.* **1987**, *26*, 715–724.
26. Lacy, W.B.; Rowlen, K.L.; Harris, J.M. *Appl. Spectrosc.* **1991**, *45*, 1598.
27. Pemberton, J.E.; Sobocinski, R.L.; Sims, G.R. *Appl. Spectrosc.* **1990**, *44*, 328.
28. Burt, D.J. *Nucl. Instrum. Methods Phys.* **1991**, *A305*, 564.
29. Chandler, E.C.; Bredthauer, R.A.; Janesick, J.R.; Westphil, J.A.; Gun, J.E. *Proc. SPIE* **1990**, *1242* 27.
30. Geary, J.C. *Proc. SPIE* **1992**, *1439*, 159.

31. CC200 Operating Manual, Photometrics Ltd., Tucson AZ, Appendix E.
32. Epperson, P.M.; Denton, M.B.; *Anal. Chem.* **1989**, *62*, 1513.
33. Sweedler, J. V.; Bilhorn, R. B. Specialized readout modes and spectrometers, in *Charge Transfer Devices for Chemistry*; J. V. Sweedler, K. L. Ratzlaff, M. B. Denton, Eds.; VCH: New York, 1993.
34. Sweedler, J.V.; Shear, J.B.; Fishman, H.A.; Zare, R.N.; Scheller, R.H. *Anal. Chem.* **1991**, *63*, 496.
35. Sweedler, J.V.; Shear, J.B.; Fishman, H.A.; Zare, R.N.; Scheller, R.H. *Proc. SPIE* **1992**, *1439*, 37.
36. Bilhorn, R.B. Scanning multichannel spectrometry using a charge-coupled device in the time-delayed integration mode, U.S. Patent 5,173,748, December 1992.
37. Sweedler, J.V.; Jalkian, R.D.; Pomeroy, R.S.; Denton, M.B. *Spectrochm. Acta* **1989**, *44B*, 683.
38. Yip, W.T.; Tse, R.S. *Rev. Sci. Instrum.* **1992**, *63*, 3777.
39. Hoffman, G.G.; Menzebach, H.-U.; Oelichmann, B.; Schrader, B. *Appl. Spectrosc.* **1992**, *46*, 568.
40. Sims, G.R. Principles of charge-transfer devices, in *Charge Transfer Device Detectors in Chemistry*; J.V. Sweedler, K.L. Ratzlaff, M.B Denton, Eds.; VCH: New York, 1993.
41. Phillips, G.R.; Harris, J.M. *Anal. Chem.* **1990**, *62*, 2351.
42. Hill, W.; Rogalla, D. *Anal. Chem.* **1992**, *64*, 2575.
43. Sims, G.R.; Denton, M.B. *Opt. Eng.* **1987**, *26*, 999.
44. Sims, G.R.; Denton, M.B. *Opt. Eng.* **1987**, *26*, 1008.
45. Bilhorn, R.B.; Denton, M.B. *Appl. Spectrosc.* **1990**, *44*, 1538.
46. Carbone, J. New advances at CID Technologies, 2nd Int. Conf. on Scientific Optical Imaging, December 1992, Grand Cayman.
47. Bilhorn, R.B.; Denton, M.B. *Appl. Spectrosc.* **1989**, *43*, 1.
48. Pilon, M.J.; Denton, M.B.; Schleicher, R.G.; Moran, P.M.; Smith, S.B. *Appl. Spectrosc.* **1990**, *44*, 1613.
49. Sweedler, J.V.; Denton, M.B.; Sims, G.R.; Aikens, R.S. *Opt. Eng.* **1987**, *26*, 120.
50. Epperson, P.M.; Jalkian, R.D.; Denton, M.B. *Anal. Chem.* **1989**, *61*, 282.
51. Ratzlaff, K.L. *Anal. Chem.* **1980**, *52*, 1415.
52. Ratzlaff, K.L. *Introduction to Computer-Assisted Experimentation*; Wiley: New York; 1987; Chapter 11.
53. Jalkian, R.D.; Pomeroy, R.S., Kolczynski, J.D.; Denton, M.B.; Lerner, J.M.; Grayzel, R. *Am. Lab.* **1989**, *February*, 47.
54. Piccard, R.D.; Vo-Dinh, T. *Rev. Sci. Instrum.* **1991**, *62(3)*, 584.
55. Jalkian, R.D.; Denton, M.B. *Proc. SPIE* **1989**, *1054*, 91.
56. Karger, A. E.; Harris, J.M.; Gesteland, R.F. *Nucl. Acid Res.* **1991**, *19*, 4955.
57. Cheng, Y.-F.; Piccard, R.D.; Vo-Dinh, T. *Appl. Spectrosc.* **1990**, *44*, 755.
58. Sweedler, J.V.; Shear, J.B.; Fishman, H.A.; Zare, R.N. New develoments in multichannel fluorescence detection for capillary electrophoresis, paper 695, FACSS, Anaheim, CA, September, 1991.
59. Jalkian, R.D.; Ratzlaff, K.L.; Denton, M.B. *Proc. SPIE* **1989**, *1055*, 123.
60. Jovin, T.M.; Arndt-Jovin, D.J. *Proc. SPIE* **1992**, *1439*, 109.
61. Arndt-Jovin, D.J.; Rober-Nicoud, M.; Kaufman, S.J.; Jovin, T.M. *Science* **1985**, *230*, 247.
62. Hiraoka, Y.; Sedat, J.W.; Agard, D.A. *Science* **1987**, *238*, 36.
63. Jovin, T.M.; Arndt-Jovin, D.J. *Annu. Rev. Biophys. Chem.* **1989**, *18*, 271.
64. Herman, B.; Jacobson, K., Eds. *Optical Microscopy for Biology*; Wiley-Liss: New York, 1990.
65. Brakenhoff, G.J.; van der Voort, H.T.M.; Visscher, K. *Proc. SPIE* **1992**, *1439*, 121.
66. Masters, B.R. *Proc. SPIE* **1991**, *1448*, 98.
67. Linderman, J.J.; Harris, L.K.; Slakey, L.L.; Gross, D.J. *Cell Calcium* **1990**, *11*, 131.
68. Spring, K.R. *Scanning Microsc.* **1991**, *5*, 63.
69. Tsay, T.-T.; Inman, R.; Wray, B.E.; Herman, B.; Jacobson, K., in *Optical Microscopy for Biology*; Wiley: New York, 1990; pp. 219–233.
70. Agard, D.A.; Hiraoka, Y.; Shaw, P.; Sedat, J.W., in *Methods in Cell Biology*; D.L. Taylor, Y.L. Young, Eds.; Vol 30, Fluorescence Microscopy of Living Cells in Culture, Part B; Academic: San Diego, 1989; pp. 353–377.
71. Jackson, P.; Urwin, V.E.; Mackay, C.D. *Electrophoresis* **1988**, *9*, 330.
72. Sutherland, J.C.; Bohai, L.; Monteleane, D.C.; Mugavero, J.; Sutherland, B.M.; Trunk, J. *Anal. Biochem.* **1987**, *63*, 446.
73. Chan, K.C.; Koutny, L.B.; Yeung, E.S. *Anal. Chem.* **1991**, *63*, 746.
74. Jackson, P. *Biochem. J.* **1990**, *270*, 705.
75. Jackson, P. *Anal. Biochem.* **1991**, *196*, 238.
76. Baker, M.; Denton, M.B. Planar chromatography and electrophoresis, in *Charge Transfer Devices for Chemistry*; J.V. Sweedler, K.L. Ratzlaff, M.B. Denton, Eds.; VCH: New York, 1993.
77. McCreery, R.L. CCD array detectors for multichannel Raman spectroscopy, in *Charge Transfer Devices for Chemistry*; J.V. Sweedler, K.L. Ratzlaff, M.B. Denton, Eds.; VCH: New York, 1993.
78. Campion, A.; Perry, S. *Laser Focus World* **1990**, *August*, 113.
79. Van Duyne, R.P., in *Chemical and Biological Applications of Lasers*; L.B. Moore, Ed.; Academic: New York, 1979; Vol. 4, Chapter 4.
80. Murray, C.A.; Dierker, S.B. *J. Opt. Sci. Am.* **1986**, *3*, 2151.
81. Dierker, S.B.; Murray, C.A.; LeGrange. J.D.; Schlotter, N.E. *Chem. Phys. Lett.* **1987**, *137*, 453.

82. Schlotter, N.E.; Schaertel, S.A.; Kelty, S.P.; Howard, R. *Appl. Spectrosc.* **1988**, *42*, 746.
83. Pemberton, J.; Sobocinski, R. *J. Am. Chem. Soc.* **1989**, *111*, 432.
84. Pemberton, J.; Sobocinski, R. *Appl. Spectrosc.* **1990**, *44*, 328.
85. Packard, R.T.; McCreery, R.L. *Anal. Chem.* **1987**, *59*, 2631.
86. Wang, Y.; McCreery, R. *Anal. Chem.* **1989**, *62*, 2647.
87. Newman, C.D.; Bret, G. G.; McCreery, R.L. *Appl. Spectrosc.* **1992**, *46*, 262.
88. Skoog, D.A.; Leary, J.L., *Princ. of Instrumental Analysis, 4th Ed.*, Saunders College Publishing, Orlando, 1992, chapter 13.
89. Knoll, P.; Singer, R. Kiefer W. Applied Spectrosc., *44*, 1990, 776.
90. Singer, R.; Knoll, P.; Kiefer W. in *Proceedings of the XIth International Conference on Raman Spectroscopy*, Wiley & Sons, Chichester, 1988, p. 953.
91. Pelletier, M.J. *Appl. Spectrosc.* **1990**, *44*, 1699.
92. Pelletier, M.J. *Proc. SPIE* **1990**, *1336*, 152.
93. Williamson, J.M.; Bowling, R.J.; McCreery, R.L. *Appl. Spectrosc.* **1989**, *43*, 372.
94. Allred, C.D.; McCreery, R.L. *Appl. Spectrosc.* **1990**, *44*, 1229.
95. Barbillat, J.; Silva, E.; Roussel, B.; Howard, S.G. *Microbeam Anal.* **1991**, *88*.
96. Sims, G.R.; Griffin, F.; Lesser, M.P. *Proc. SPIE* **1989**, *1071*, 31–42.
97. Lesser, M.P.; Olszewski, E.; Sims, G.R.; Griffin, F. *Proc. SPIE* **1989**, *1071*, 43–50.
98. Batchelder, D.; Cheng, C.; Pitt, G.D. *Adv. Mate.* **1991**, *3*, 566.
99. Bowden, M.; Gardiner, D.J.; Rice, G.; Gerrard, D.L. *J. Raman Spectrosc.* **1990**, *21*, 37.
100. Treado, P.J.; Morris, M.D. *Anal. Chem.* **1989**, *61*, 723A.
101. Treado, P.J.; Morris, M.D. *Appl. Spectrosc.* **1990**, *44*, 1270.
102. Morris, M.D.; Govil, A.; Liu, K.L.; Sheng, R. *Proc. SPIE* **1992**, *1439*, 95.
103. Cosgrove, J.A.; Bilhorn, R.B. *J. Planar Chromatogr.* **1989**, *2*, 362–367.
104. Koutney, L.B.; Yeung, E.S. *Anal. Chem.* **1993**, *65*, 183.
105. Margoshes, M. *Spectrochim Acta* **1970**, *25B*, 113.
106. Margoshes, M. *Opt. Spectra* **1970**, *4*, 26.
107. Talmi, Y.; Busch, K.W. Guidelines for the selection of optoelectronic image detectors for low-light level applications, in *Multielement Imaging Detectors*; Y. Talmi, Ed.; ACS Symposium Series 236; American Chemical Society, Washington, D.C., 1983; Vol. 2.
108. Busch, K.W.; Busch, M.A. *Multielement Detection Systems for Spectrochemical Analysis*; Wiley Interscience: New York, 1990.
109. Harrison, G.R. *J. Opt. Am.* **1949**, *39*, 552.
110. Pomeroy, R.S.; Jalkian, R.D.; Denton, M.B. *Appl. Spectrosc.* **1991**, *45*, 1120.
111. Scheeline, A.; Bye, C.A.; Miller, D.L.; Rynders, S.W.; Owen, R.C. *Appl. Spectrosc.* **1991**, *45*, 334.
112. Bilhorn, R.B. *Proc. SPIE* **1991**, *1448*, 74.
113. Krupa, L.B.; Leominster, R.; Owen, C. A two-dimensional spectrometer, U.S. Patent 4,995,211, February 1991.
114. Barnard, T.W.; Crockett, M.I.; Ivaldi, J.C.; Lundberg, P.L. *Anal. Chem.* **1993**, *65* in press.
115. Barnard, T.W.; Crockett, M.I.; Ivaldi, J.C.; Lundberg, P.L.; Yates, D.A.; Levine, P.A.; Sauer, D.J. *Anal. Chem.* **1993**, *65* in press.
116. Barnard, T. Atomic spectroscopic CCD detectors," 2nd Int. Conf. on Scientific Optical Imaging, December 1992, Grand Cayman.
117. Pomeroy, R.S.; Kolczynski, J.D.; Sweedler, J.V.; Denton, M.B. *Mikrochim. Acta* **1989**, *III*, 347.
118. Pomeroy, R.S.; Sweedler, J.V.; Denton, M.B. *Talanta* **1990**, *37*, 115.
119. Pomeroy, R.S.; Kolczynski, J.D.; Denton, M.B. *Appl. Spectrosc.* **1991**, *45*, 1111.
120. Hsiech, C.; Petrovic, S.C.; Pardue, H.L. *Anal. Chem.* **1990**, *62*, 1983.
121. Harnly, J. *Spectrochim. Acta* **1993**, *48B*, in press.
122. Harnly, J. *J. Anal. Atomic. Spectrosc.* **1993**, *8*, in press.
123. Harnly, J. Continuum atomic absorption using array detector technology, 2nd Int. Conf. on Scientific Optical Imaging, December 1992, Grand Cayman.
124. Kolczynski, J.D.; Pomeroy, R.S.; Jalkian, R.D.; Denton, M.B. *Appl. Spectrosc.* **1989**, *43*, 887.
125. Monnig, C.A.; Gebbert, B.D.; Marsall, K.A.; Hieftje, G.M. *Spectrochim. Acta* **1990**, *45B*, 261.
126. Monnig, C.A.; Gebbert, B.D.; Hieftje, G.M. *Appl. Spectrosc.* **1989**, *43*, 577.
127. Mork, B.J.; Scheeline, A. *Spectrochim. Acta* **1989** *44B*, 1297.
128. Bargigia, A.; Emolumento, E.; Liguori, C.; Paganini, E.; Parini, U.; Piemontese, V.; Tondello, G. *Meas. Sci. Technol.* **1992**, *3*, 992.
129. Lumb, D. *Nucl. Instrum. Methods Phys. Res. A* **1986**, *247*, 309.
130. Bross, A.D.; Clegg, D.B. *Nucl. Instrum. Method Phys. Res. A* **1987**, *260*, 80.
131. Rodricks, B.F. *Rev. Sci. Instrum.* **1989**, *60*, 2586.
132. Strauss, M. *IEEE Trans. Nucl. Sci.* **1987**, *NS-34*, 389.
133. Mantus, D.S.; Vallaskovic, G.A.; Morrison, G.H. *Anal. Chem.* **1991**, *63*, 788.
134. Eikenberry, E.F.; Tate, M.W.; Belmonte, A.L.; Lowrance, J.L.; Bilderback, D.; Gruner, S.M. *IEEE Trans. Nucl. Sci.* **1991**, *NS-38*, 110.
135. Bonse, U.; Nusshardt, R.; Busch, F.; Pahl, R.; Johnson, QC.; Kinney, J.H.; Saroyan, R.A.; Nichols, M.C. *Rev. Sci. Instrum.* **1989**, *60*, 2478.
136. Koppel, L.N. *Rev. Sci. Instrum.* **1977**, *48*, 669.
137. Peckerar, M.C.; Baker, W.D.; Nagel, D.J. *J. Appl. Phys.* **1977**, *48*, 2565.
138. Stern, R.A.; Liewer, K.; Janesick, J.R. *Rev. Sci. Instrum.* **1983**, *54*, 198.

139. Janesick, J.R.; Elliott, T.; Collins, S.; Daud, T.; Campbell, D.; Garmire, G. *Opt. Eng.* **1987**, *26*, 156.
140. Janesick, J.R.; Elliott, T.; Bredthauer, R.; Chandler, C. *X-ray instrumentation in astronomy* Golub, L. Ed., SPIE, Bellingham WA, 1988, 1.
141. Fano, U. *Phys. Rev.* **1947**, *72*, 26.
142. Lumb, D.H. *Nucl. Instrum. Methods Phys. Res. A* **1990**, *290*, 559.
143. Clarke, R. *Nucl. Instrum. Methods Phys. Res. A* **1990**, *290*, 117.
144. Ellila, M.; Pollari, K. *Nucl. Instrum. Methods Phys. Res. A* **1990**, *288*, 267.
145. SLD Colloboration, Technical Proposal, SLAC Report 273, 1984.
146. Andert, K.; Schälike, W.; Nölting, B.; Pittelkou, R.; Wetzel, R.; Snatzike, G. *Rev. Sci. Instrum.* **1991**, *62*, 1912.